Chapter 1

Introduction

With the advent of technology, dimensions of semiconductor devices and integrated circuits are decreasing. This miniaturization is accompanied with new and advanced functions which have made electronics more reliable, faster, more powerful and less expensive. The comparison of latest laptops with the bulky computer makes the picture clear. The demand of small sized products with improved qualities is driving the research towards further lowering of device dimensions. Accordingly sizes have shrunk and there are convincing indications that we are entering a new era, namely the age of nano from the age of micro. The term micro refers to the size of a device's active zone which is in micrometers (10^-6m), e.g. the channel length of a field effect transistor or the thickness of the gate dielectric. Nano refers to the typical geometrical dimension of an electronic device which is in nanometer (10^-9m or one billionth of a meter) that is 1000 times less than micrometer.

Nanotechnology is the fabrication of nanomaterials and to make good use of their improved physical, chemical or biological properties to develop superior materials, engineering processes and symmetric products. Nanoparticles are the building blocks of nanotechnology. They can be just about anything whose dimensions are on the nanometer scale while nanocrystals usually are the nanometric sized metals, semiconductors or insulator. It is basically considered as a three-dimensional particle box in which photon absorption and annihilation of some elementary excitations in an electron subsystem occurs. These excitations are described in terms of quasi particles known for bulk crystals, that is, electrons, holes and excitons [1].

Quantum dot is a term applied to semiconductor nanocrystals in a size limit whose volume is smaller than the volume defined by the exciton Bohr radius of that particular semiconductor. It is an ideal nanocrystal and can be considered as a bit of a crystal with a spherical or cubic shape. The behavior of quantum dots is dictated by quantum mechanics. They

behave as artificial atoms. They can confine single or few electrons inside them where the electrons occupy discrete energy levels.

1.1 Quantum confinement

The reason behind such extraordinary expectations from nanomaterials lies behind their properties. They are different from their bulk counterparts in the degree of freedom of the particles inside them. In a bulk material, the particles are free to move in all the three dimensions whereas in low dimensional structures, the movement of the particle is confined or restricted in one or more dimensions. At the nanometer scale of size, classical description of solid state properties breakdown and quantum mechanics comes into the picture. Quantum confinement approach explains a lot of features connected with these low dimensional structures. Due to confinement of charge carriers inside a potential in nanomaterials, the electronic structure of bulk and nanostructure of same material differs. The electronic structure of bulk semiconductors is characterized by delocalized state and by quasi continuous spectrum of energies in the conduction and valance bands, while in semiconductor nanostructures, when the charge carriers are confined in the small regions of space in the range of few tens of nanometers or below, the energy spectrum is profoundly affected by the confinement, acquiring mainly following characteristics [2, 3, 4],

- An increase in band gap.
- The allowed energies becomes discrete in zero dimensional systems and forms mini bands in one and two-dimensional systems.
- The particle shows a non vanishing probability and moves outside the confined walls. In particular, it has a chance of penetrating a neighbour potential with high walls. So there is a possibility of so-called tunneling.
- There is enhanced volume-normalized oscillator strength of exciton features. This arises because the oscillator strength becomes concentrated over sharp electron-hole transitions, rather than being distributed over a continuum of states as for the case of bulk semiconductors. There is enhanced exciton nonlinearity and a reduction in optical power required for the optical saturation relative to the bulk semiconductors.

- There is enhanced exciton nonlinearity and a reduction in optical power required for optical saturation relative to the bulk semiconductors.

1.2 Nanoparticle

In nanotechnology a particle is defined as a small object that behaves as a whole unit in terms of its transport and properties. Particles are further classified according to size in terms of diameter; fine particles cover a range between 100 and 2500nm. On the other hand, ultrafine particles are sized between 1 and 100 nanometers. Similar to ultrafine particles, nanoparticles are sized between 1 and 100 nanometers. Nanoparticles may or may not exhibit size-related properties that differ significantly from those observed in fine particles or bulk materials. Although the size of most molecules would fit into the above outline, individual molecules are usually not referred to as nanoparticles.

Nanoparticle research is currently an area of intense scientific interest due to a wide variety of potential applications in biomedical, optical and electronic fields.

1.3 Classification of nanoparticles

The term of nanomaterials covers various types of nanosturctured materials which possess at least one dimension in the nanometer range. There are two ways, depending on which nanoparticles can be classified. First on the basis of their properties and second on the basis of reduction in their dimensions,

1.3.1 Metal and Semiconductor nanoparticles

Depending on the properties nanoparticles can be classified into two types. These are metal nanoparticles and semiconductor nanoparticles.

Metal nanoparticles are generally synthesized by sol-gel method, in which we use capping agents to prevent aggregation for controlling the size. The quantum confinement in metal nanoparticles occurs when the electrons motion is limited by the size of the nanoparticle. The electronic energy levels of the particle around the Fermi level are affected only for very small sizes in these nanoparticles. These nanoparticles show a very weak photoluminescence but exhibit UV-visible absorption which is determined by the surface Plasmon resonance, which is size and shape dependent. Metal nanoparticles are generally used as catalyst in the reaction processes.

Semiconductor nanoparticles are synthesized with a variety of chemical methods to produce desired size, shape and structure. In these nanoparticles quantum confinement occurs when the radius of the nanoparticles is comparable to the exciton's Bohr radius. These nanoparticles show strong luminescence and visible spectra. The UV-visible absorption is determined by the band edge transition, which is strongly size and shape dependent (band gap energy increases as the size decreases) and hence highly tunable. Theses nanoparticles have application in various fields due to their advanced properties [5].

1.3.2. Low dimensional structures (on the basis of their dimensions)

The structures, in which the movement of the particles is restricted in either one, two or three dimensions, are called low dimensional structures. Nanosize effect occurs even if only one dimension is of nanometer size. This confinement can be obtained by creating a structure whose dimension (one, two or three) are greater than the lattice constant a_L and are comparable or less than the length parameters of the quasiparticles, i.e. de Broglie wavelength of an electron and hole (λ_e and λ_h respectively) and the exciton Bohr radius a_B [1]. It is possible, because in most semiconductors, the de Broglie wavelength and the exciton Bohr radius are much larger than the lattice constant. In these structures, the elementary excitations will experience quantum confinement and thus have finite motion along the confinement axis and infinite motion in other directions. When the size is restricted in one dimension, we get a two-dimensional structure called quantum well. In case the confinement is in two dimensions, we get a one dimensional structure called quantum wire and finally, if the motion of the electrons, holes and excitons is

restricted in all the three dimensions then we obtained a quasi-zero dimensional system, the so-called quantum dot.

Quantum confinement effect present in these three categories of low dimensional structure can be explained in terms of density of states obtained for these systems. Density of states is the number of electronic states per unit volume per unit range around an energy *E*. it is denoted by *N (E). N (E) dE* denotes the number of states in a unit volume in an energy interval *dE* around an energy *E*. *N (E)* is given by [6],

$$N(E) = \frac{\sqrt{2}m^{3/2}(E - U_0)^{1/2}}{\pi^2\hbar^3} \quad (1.1)$$

Where, U_0 is some background potential and *m* is the electron mass. Important physical properties such as optical absorption, thermal transport etc. are intimately depend upon density of states.

1.3.2.1 Quantum well

A quantum well is a particular kind of heterostructure in which one thin "well" layer is surrounded by two "barrier" layers. Both electrons and holes see lower energy in the "well" layer, hence the name (by analogy with a "potential well"). This layer, in which both electrons and holes are confined, is so thin (typically about 100 Å or about 40 atomic layers) that we cannot neglect the fact that the electron and hole are both waves. In fact, the allowed states in this structure correspond to standing waves in the direction perpendicular to the layers. Because only particular waves are standing waves, the system is quantized. The difference between the potential in the well and in the barriers defines the confining potential *U(r)* which is commonly approximated as the square potential depending upon the coordinate *x*. Schrodinger wave equation for this case is given by[2, 7],

$$\frac{\partial^2\Psi(x)}{\partial x^2} + \frac{2m}{\hbar^2}[E - U(x)]\Psi(x) = 0 \quad (1.2)$$

The solution of the above equation will have the form,

$$E_{kn} = \frac{\hbar^2 k^2}{2m} + E_n^x \quad (1.3)$$

Where, k is the propagation constant and n= 1, 2….. The density of states is then given by,

$$N(E) = A \sum_{n} \emptyset(E - E_n^x) \tag{1.4}$$

Where, A is a constant, and $\emptyset(x)$ is equal to 1, if x>0 and 0 otherwise. Thus the DOS (figure 1.1) in a two dimensional system is a staircase function with a discontinuity at each E_n^x whereas in a 3D system the DOS becomes a continuous function of energy. It is also important to point out that the 2D DOS is finite at the bottom of the lowest sub band whereas the 3D one is equal to zero, which has fundamental consequence on the properties of 2D systems, for example the gain of quantum well lasers.

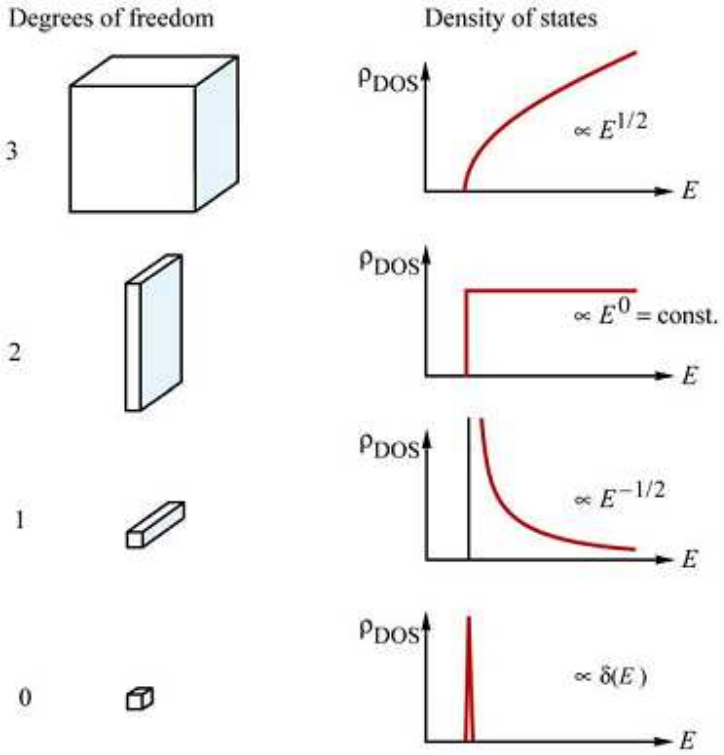

Figure 1.1 Electronic densities of states of semiconductors with 3, 2, 1 and 0 degree of freedom

1.3.2.2 Quantum wire

Quantum wire is a 1D structure in which motion of the particle is free in one direction and restricted in other two directions. So, here we have confinement in two directions. (e.g. *x* and *y*). Using the square potential *U(x, y)* in *y* and *z* directions we have the solution of the Schrodinger equation [7],

$$E_{kn_xn_y} = \frac{\eta^2 k^2}{2m} + E_{n_x}^x + E_{n_y}^y \quad (1.5)$$

The first term in the right hand side of the above equation gives the kinetic energy of the carriers along the wire axis. The DOS is given by,

$$N(E) = B \sum_{n_x n_y} (E - E_{n_x}^x - E_{n_y}^y)^{1/2} \quad (1.6)$$

Where, B is a constant and n_x and n_y = 1, 2…. The DOS (figure 1.1) is equal to zero when E<$E_{n_x}^x + E_{n_y}^y$ for n=1. Thus the quantum confinement leads to an opening of the band gap like in 2D systems but the 1D DOS is highly peaked, since it represents singularities at each value of $E_{n_x}^x + E_{n_y}^y$. The 1D sub bands are often referred to as channels when discussing transport phenomenon of quantum wires.

1.3.2.3 Quantum dots

In quantum dot, confinement takes place in all the three directions of space. The electronic spectrum in this case consists of discrete levels, like in isolated atoms. Now the square potential is in all three directions. The eigen values in this case is given by [8],

$$E_{n_xn_yn_z} = E_{n_x}^x + E_{n_y}^y + E_{n_z}^z \quad (1.7)$$

The DOS (figure 1.1) consists of δ functions at discrete energies,

$$N(E) = 2 \sum_{n_x n_y n_z} \delta (E_{n_x}^x + E_{n_y}^y + E_{n_z}^z) \quad (1.8)$$

Where, n_x, n_y and n_z= 1, 2….. In quantum dots or 0D systems, the confinement not only widens the band gap, but it also converts the continuous energy bands into discrete levels.

1.4 Height calculation of nanoparticles

Lu *et al.* [9] in their paper have given a relationship between height and band gap under quantum confinement circumstances. It is given by,

$$E = E_g + \frac{\hbar^2\pi^2}{2}\left(\frac{1}{m_e^*}+\frac{1}{m_h^*}\right)\left(\frac{1}{h^2}+\frac{1}{d^2}\right) - E_{ex} \quad (1.9)$$

Where, E_g is the bulk band gap of the material, m_e^* & m_h^* are the electron and hole effective masses, h is the height of the nanodot, d is the diameter of the nanodot and E_{ex} is the bulk excitonic energy of the material.

1.5 General properties of the nanoparticles/nanomaterials

Nanomaterials have the structural features in between of those of atoms and the bulk materials. While most micro structured materials have similar properties to the corresponding bulk materials, the properties of materials with nanometer dimensions are significantly different from those of atoms and bulks materials. This is mainly due to the nanometer size of the materials which render them:

- Large fraction of surface atoms
- High surface energy
- Spatial confinement
- Reduced imperfections

These characteristics do not exist in the corresponding bulk materials. Due to their small dimensions, nanomaterials have extremely large surface area to volume ratio, which makes a

large fraction of atoms of the materials to be the surface or interfacial atoms, resulting in more "surface" dependent material properties. Especially when the sizes of nanomaterials are comparable to Debye length, the entire material will be affected by the surface properties of nanomaterials. This in turn may enhance or modify the properties of the bulk materials. For example, metallic nanoparticles can be used as very active catalysts. Chemical sensors from nanoparticles and nanowires enhanced the sensitivity and sensor selectivity. The nanometer feature sizes of nanomaterials also have spatial confinement effect on the materials, which bring the quantum effects.

The quantum confinement of nanomaterials has profound effects on the properties of nanomaterials. The energy band structure and charge carrier density in the materials can be modified quite differently from their bulk counterpart and in turn will modify the electronic and optical properties of the materials.

For example, lasers and light emitting diodes (LED) from both of the quantum dots and quantum wires are very promising in the future optoelectronics. High density information storage using quantum dot devices is also a fast developing area. Reduced imperfections are also an important factor in determination of the properties of the nanomaterials.

Apart from the quantum confinement effect classical effect also plays an important role in affecting the properties of a material when it comes to the nanoscale dimension. This is due to the fact that the mean free path for inelastic scattering becomes comparable with the size of the system leading to a reduction with scattering effects.

Nanostructures and nanomaterials favors of a self-purification process in that the impurities and intrinsic material defects will move to near the surface upon thermal annealing. This increased materials perfection affects the properties of nanomaterials. For example, the chemical stability for certain nanomaterials may be enhanced, the mechanical properties of nanomaterials will be better than the bulk materials. The superior mechanical properties of carbon nanotubes are well known. Due to their nanometer size, nanomaterials are already known to have many novel properties. Many novel applications of the nanomaterials rose from these novel properties have also been proposed.

1.5.1 Mechanical properties

Due to the nanometer size, many of the mechanical properties of the nanomaterials are modified to be different from the bulk materials including the hardness, elastic modulus, fracture toughness, scratch resistance and fatigue strength etc. An enhancement of mechanical properties of nanomaterials can result due to this modification, which are generally results from structural perfection of the materials. The small size either renders them free of internal structural imperfections such as dislocations, micro twins, and impurity precipitates or the few defects or impurities present cannot multiply sufficiently to cause mechanical failure. The imperfections within the nano-dimension are highly energetic and will migrate to the surface to relax themselves under annealing, purifying the material and leaving perfect material structures inside the nanomaterials. Moreover, the external surfaces of nanomaterials also have less or free of defects compared to bulk materials, serving to enhance the mechanical properties of nanomaterials. The enhanced mechanical properties of the nanomaterials could have many potential applications both in nano scale such as mechanical nano resonators, mass sensors, microscope probe tips and nano tweezers for nano scale object manipulation, and in macro scale applications structural reinforcement of polymer materials, light weight high strength materials, flexible conductive coatings, wear resistance coatings, tougher and harder cutting tools etc.

1.5.2 Thermal properties

The recent advances of nanotechnologies in the past decades have resulted in the burst of promising synthesis, processing and characterization technologies, which enables the routine production of a variety of nanomaterials with highly controlled structures and related properties. By controlling the structures of nanomaterials at nano scale dimensions, the properties of the nanostructures can be controlled.

Heat is transported in materials via two different mechanisms. These are:-

1. Free electrons

2. Lattice vibrations (phonons)

In metals the electron mechanism is of thermal transport is significantly more efficient then phonon process due to the fact that metal possess high no of electrons and they are not as easily scattered. But in case of nanomaterials phonons are the main mechanism of the thermal transport due to the lack of availability of the free electrons and because phonon scattering is much more efficient.

As the dimension goes down to nano scales, the size of the nanomaterials is comparable to the wavelength and the mean free path of the photons, so that the photon transport within the materials will be changed significantly due the photon confinement and quantization of photon transport, resulting in modified thermal properties[10]. For example, nanowires from silicon have a much smaller thermal conductivities compared to bulk silicon. The special structure of nanomaterials also affects the thermal properties leaving high anisotropy in the heat transport in the materials. The in interfaces are also very important factor for determine the thermal properties of nanomaterials. Generally, the internal interfaces impede the flow of heat due to photon scattering. At interface or grain boundary between similar materials, the interface disorder scatters phonons, while as the differences in elastic properties and densities of vibrational states affect the transfer of vibrational energy across interfaces between dissimilar materials. As a result, the nanomaterials structures with high interfaces densities would reduce the thermal conductivity of the materials. These interconnected factors joined together to determine the special thermal properties of the nanomaterials.

1.5.3 Electrical properties

The electrical properties of nanomaterials highly depend upon quantum confinement and classical effects. So, electrical conductivity for different types of nanomaterials is different.

(a) Three-Dimensional nanomaterials

In a 3-D nanomaterial all three spatial dimensions are above nanoscale so these two effects can be ignored.

Bulk nanocrystalline materials exhibit high grain boundary area to volume ratio leading to increase in the electron scattering. As a result nanosize grain tends to reduce electrical conductivity.

(b) Two-Dimensional nanomaterials

In a 2-D nonmaterial confinement occurs along the thickness direction. As the thickness is reduced to the nanoscale, the wave function of the electrons is limited to a very specific value along the cross section. This is because only those electron wavelengths, which are multiple integers of thickness, will be allowed. In other words there is a reduction in no of energy states available for the electron conduction along thickness direction. The electrons became trapped in a well called potential well of width equal to the thickness. The effects of confinement on the energy states for a 2-D nanomaterial with thickness of nanoscale can be written as [11],

$$En = \left\lfloor \frac{\pi^2 \hbar^2}{2ml^2} \right\rfloor n^2 \qquad (1.10)$$

Where,

$\hbar = \frac{h}{2\pi}$

m= mass of electron

L = length of the well

n = principle quantum number

Thus carriers are free to move along the plane of sheet. Thus total energy of carrier has two components-

(a) Term related to confinement dimension
(b) Term associated with unrestricted motion along the in plane dimension.

Let Z direction be the thickness direction and X, Y are in-plane direction in which electrons are delocalized. So unrestricted motion can be characterized by two wave vectors Kx and Ky which are related to the electron's momentum along the X and Y direction respectively such that:-

$$Px = \hbar Kx \tag{1.11}$$

$$Py = \hbar Ky \tag{1.12}$$

So the energy corresponding to these delocalized electrons i.e. Fermi energy is given by,

$$Ef = \left\lfloor \frac{\hbar^2}{2m} \right\rfloor Kf^2 \tag{1.13}$$

Thus total energy of electron (due to confinement and restricted motion) in a 2-D nanomaterial with thickness is given by,

$$En = \left\lfloor \frac{\sqcap^2 \hbar^2}{2ml^2} \right\rfloor n^2 + \left\lfloor \frac{\hbar^2}{2m} \right\rfloor Kf^2 \tag{1.14}$$

Since the electron states are confined along the thickness, the electron momentum is relatively only in in-plane direction. As a result scattering by phonons and impurities occurs in in-plane leading to 2-D electron conduction. But large amount of grain boundary area in 2-D nanomaterials provides an additional source of in-plane scattering, thus providing better electrical conductivity.

(c) One-Dimensional nanomaterials

In 1-D nanomaterials confinement occurs in the two directions that is unrestricted motion is only along the long axis of nanotube/nanorod/nanowire. Thus for a 1-D nanomaterials, the energy states depend upon two quantum no n_y andn_z [11]. Thus,

$$E_{n_{y n_z}} = \left\lfloor \frac{\pi^2 \hbar^2}{2ml^2} \right\rfloor {n_y}^2 + \left\lfloor \frac{\pi^2 \hbar^2}{2ml^2} \right\rfloor {n_z}^2 \tag{1.15}$$

Thus electronic states of a 1-D nanomaterial do not exhibit a single energy band but instead spread into the sub-bands. Because of the confinement, the nanoscale dimensions of 1-D acts as reflectors; not allowing the electrons to exit the surfaces. In addition to that scattering by the phonons and impurities restricted to the long axis of the tube, despite the fact that the boundary scattering is more pronounced due to high surface to volume ratio of 1-D nanomaterials, providing good electrical conductivity as in the case if CNT.

1.5.4 Optical properties

One of the most fascinating and useful aspects of nanomaterials is their optical properties. Applications based on optical properties of nanomaterials include optical detector, laser, sensor, imaging, phosphor, display, solar cell, photo catalysis, photo electrochemistry and biomedicine. Many of the underlying principles are similar in these different technological applications that span a variety of traditional disciplines including chemistry, physics, biology, medicine, materials science and engineering, electrical and computer science and engineering.

The optical properties of nanomaterials depend on parameters such as feature size, shape, surface characteristics, and other variables including doping and interaction with the surrounding environment or other nanostructures. The simplest example is the well-known blue-shift of absorption and photoluminescence spectra of semiconductor nanoparticles with decreasing particle size, particularly when the size is small enough. For semiconductors, size is a critical parameter affecting optical properties [1].

In case of metallic nanoparticles, color may change with size due to surface plasmon response. The indirect band gap materials, like germanium and silicon, which do not emit light in their bulk form, emits light as their size is reduced to nanometer range. Due to this these indirect band gap materials can also be used in the light emitting applications. Sometimes in nanoparticles there is enhanced volume normalized oscillator strength of excitons gives rise to non linear optical properties.

1.5.5 Magnetic properties

The basic magnetic properties of a material are often described by a B-H curve (B Magnetic flux density, H Magnetic field strength). Materials either slightly reject magnetic fields

(diamagnetism) or reinforce them (paramagnetism). A limited set of materials (Fe, Co, Ni, and some transition metal oxides) exhibit ferromagnetism, i.e. spontaneous alignment of atomic spins. Ferromagnetism of bulk materials disappears and transfers to super-paramagnetism in the nanometer scale due to huge surface energy. Also the disappearance of magnetization on removal of external magnetic field depends upon particle size. The magnetization of the material responds promptly with the external magnetic field when the particle is small enough but it decreases with increase in size. Due to this phenomenon, gold nanoparticles which are stable as bulk shows catalytic behavior as nanoparticles.

1.6 General application of nanomaterials

The application of nanomaterials is almost everywhere. Starting from medical to engineering, from plastic to metals, from painting colours to cosmetics, almost all the products are influenced by its application. It has touched all the field of sciences, which are benefitted by its advanced properties. The first quantum dot was probably made inside glass matrix while making colored glasses.

The localized Plasmon response of metallic nanoparticles is used in bio and chemical sensors for sensing the affinity between molecules (affinity biosensors) and for providing vibration spectrum in Raman sensor [12]. Metal nanoparticles are used in various field, for example Ag nanoparticles paste is developed to be used to prepare fine electronic circuit pattern by screen printing [12]. Nanoparticles have been designed for oral drug delivery of peptide-based pharmaceuticals which were different to take earlier as they were decomposed easily by proteolytic enzymes existing in the body. This problem is solved after using nanoparticles for the delivery. They have the ability to protect the drugs from harsh gastrointestinal environment and also translocates it to intestinal membrane. Use of nanomaterials as phosphorus is widespread now. Many diagnosis tests in biomedical field are giving fast and accurate results after incorporation of nanoparticles [13]. Optical engineering of these laboratory tests has evolved after use of fluorescent biomarkers like quantum dots. Bio-imaging using quantum dots gives much better results compared to the conventional fluorescence dyes. The strong intensity of the

fluorescent makes it possible to detect immunological reaction by the small amount of the antibody by using quantum dots labeling [12]. Carbon nanotube (CNT) is one of the nanomaterials which have vast application including electron emission source of field emission display (FED), cantilever of scanning electron microscope (SEM) etc. Recently, Xiao *et al.* [14] have made practical carbon nanotube thin film loudspeakers, which possess the merits of nanometer thickness and are transparent, flexible, stretchable, and magnet-free. Bright phosphorus is developed by incorporating semiconductor nanoparticles in glass substrate. Ultrafine particles of titanium oxide are used in surfactant lotions from 1980's. The absorption and scattering phenomena of titanium oxide and zinc oxide are used to protect the skin from ultra-violet rays. Ultra fine pressure emulsification is used to reduce the size of the active ingredients to nano range which are smaller than the gaps in skin cells, to improve the permeability and absorbability.

In recent years, a large variety of nanometer scale devices have been investigated for using them in place of semiconductor devices, as the nanometer scale devices are more suitable physically and economically. In this context, a renaissance may be expected in the field of computer memory with the introduction of memristor (resistor with memory), having hysteresis effect. A new type of ultra dense non-volatile random access memory (RAM), could be created where bits are stored as the 'on' and 'off' states of a series of memristor. Memristor according to Leon Chua [16] is the fourth two-terminal circuit building passive element (the other three being resistor, inductor and capacitor) which, according to him, exists due to the sake of completeness of the circuit theory.

1.7 Zinc sulfide (ZnS)

Zinc sulfide is a chemical compound with the formula ZnS. Zinc sulfide is a white to yellow colored powder or crystal. It is typically encountered in the more stable cubic form, known also as zincblende or sphalerite. The hexagonal form is also known both as a synthetic material and as the mineral wurtzite. A tetragonal form is also known as very rare mineral polhemusite (Zn,Hg)S. Both sphalerite and wurtzite are intrinsic, wide-band gap semiconductors

[17]. ZnS, well-known direct band gap II–VI semiconductor, is promising materials for photonic, optical, and electronic devices. Nanosturctured materials have lent a leading edge to the next generation technology due to their distinguished performance and efficiency for device fabrication. As one of the most suitable materials with size and dimension dependent functional properties, wide band gap semiconducting ZnS nanostructure has attracted particular attention in recent years. For example, this material has been assembled into nanometer-scale visible-light-blind ultraviolet (UV) light sensors with high sensitivity and selectivity, in addition to other applications such as field emitters and lasers. Their high-performance characteristics are particularly due to the high surface-to-volume ratios (SVR) and rationally designed surfaces.

Table 1.1 Physical properties of fundamental ZnS structure

SN	PROPERTY	ZnS	
		Zinc Blende	Wurtzite
1	Lattice parameters (at 300k)	a= 0.541nm	a= 0.3811 nmc= 0.6234nm
2	Density (at 300k)	4.11 $g.cm^{-3}$	3.98 $g.cm^{-3}$
3	Dielectric constant	8.9	9.6
4	Refractive index	2.368	2.356/2.378
5	Energy Gap E_g (at 300k)	3.68	3.91
6	Exciton binding energy (meV)	39	39
7	Positions of UV emissions	330-345nm	330-345nm

1.7.1 Review of experimental research works on nanocrystalline ZnS

ZnS is a II-VI group semiconductor material having wide band gap which becomes wider as we deal with the nanostructure of these materials. These materials are suitable for applications in devices with optical range from UV to visible region. Becker *et al*. [19] synthesized colloidal ZnS dispersions and studied its photoluminescence properties. They reported the high luminescence of ZnS and inferred that the photo physical properties of ZnS are very sensitive to

surface effects. Yang *et al*. [20] synthesized ZnS nanocrystals in polymer matrix and studied the properties through photoluminescence and electroluminescence. The absorption and luminescence of ZnS nanoparticles of different size is studied in detail by Chen *et al*. [21] they observed two absorption bands in their absorption spectra. They considered the origin of the additional band from the surface states. ZnS nanoparticles without any stabilizer were prepared by Xu *et al*. [22] they studied the properties of the prepared sample by various characterization techniques. Passler *et al.* [23] studied the temperature dependence of exciton peak energies of epitaxial films of II-VI materials (including ZnS) grown by molecular beam Epitaxy (MBE). Qadri *et al*. [24] reported a significant reduction in the zincblende to wurtzite phase transition temperature in nanometer sized ZnS particles as compared to the bulk state. Photo physical properties of ZnS Nanoclusters, synthesized by wet chemical route, were studied in detail by Kumbhojkar *et al*. [50]. They studied the effects of various defects levels on the luminescence behavior of ZnS nanoparticles. Nanobelts, nanocombs and nanowindmills of wurtzite ZnS were synthesized and studied by Christopher *et al.* [26]. Chakraborty *et al.* [27] prepared nanoscale semiconductor particles of ZnS in polymer surfactant gel matrix. They infer that absorption and emission characteristics substantially depend upon environment in which the particles were dispersed or embedded. ZnS nanoparticles were studied for field emission devices by Ghosh *et al.* [28]. Ding *et al.* [29] controlled the deposited ZnS nanostructures being zincblende phase, wurtzite phase or a mixture by adjusting the synthesis conditions through a vapour-liquid-solid process. Rathore *et al.* [30] reported the energy increase band gap of chemically synthesized ZnS nanoparticles with increase in molar concentration of reactant solution. Very recently in 2009, the luminescence of undoped and Cu doped ZnS quantum dots have been studied by Nath *et al*. [31]. They used zeolite as a matrix, which plays a key role in controlling the size of the quantum dots.

Bhargava *et al*. [13] was the first to study the Mn doped ZnS nanocrystals. Their work revealed both a high luminescent efficiencies and drastic change in spontaneous decay rate of Mn^{2+} ions embedded in nanocrystals, as compared with ZnS bulk. They opened the research in doped nanocrystals. Khosravi *et al*. [33] studied the structural and optical properties of Mn doped ZnS nanocrystals synthesized by aqueous method. Huang *et al.* [34] prepared ZnS:Cu nanocrystals in polymer networks using chemical route. The photoluminescence and electroluminescence of Cu doped ZnS nanocrystals was also studied by Que *et al.* [35]. They

prepared their samples in an inverse micro emulsion by the hydrothermal technique. They also studied the I-V curves of the Cu doped ZnS nanocrystals. The luminescence quenching in ZnS nanoparticles due to Fe and Ni doping was studied by Borse *et al.* [36]. Structural, optical and luminescence properties of Cu doped ZnS thin films were studied as a function of dopant concentration by Jayanthi *et al.* [37]. Surface passivation and photo luminescence of Mn doped ZnS nanocrystals are studied by Yang *et al.* [38].

1.7.2 Review of application of ZnS

ZnS is II-VI semiconductor material is used in many applications primarily for its luminescent properties. It has a wide band gap of 3.68eV, a small exciton Bohr radius of 2.5nm and an exciton binding energy of 40meV, which is quite high [17]. Cu doped ZnS bulk is an inorganic material used for light emitting diodes (LED). Owing to its wide band gap, it is used in violet and blue regions. Huang et al. has fabricated light emitting diode with ZnS:Cu nanocrystals as the emitting layer of the Led. Que *et al.* [35] has studied the current-voltage characteristics of Cu doped ZnS polymer composite single layer structure electroluminescence (EL) device. They reported ear inversion symmetry of the characteristic and concluded that the direction of the applied bias is not important for the electrical properties. ZnS quantum dots have been grafted to rod-shaped viruses through peptide intermediaries which at high concentration assemble into a thin transparent film that can be picked with tweezers. These films in which a viral rod pack together likes liquid crystal find use as high density storage media or in displays. ZnS has become a useful material for bio-imaging applications. CdSe quantum dots surface-conjugated with ZnS are known to have high photo stabilities and as a result they can be traced much longer when used for luminescent tagging [12]. In addition with the photo stability, brightness of III-V materials also increases when their surfaces are conjugated with ZnS. Warad *et al*. [40] has reported the synthesis of Mn doped ZnS phosphors, capped with chitosan. Chitosan is a bio-compatible polymer and Warad show the use of above particles in biological labeling.

1.8 Motivation of the present work

As ZnS, a II-VI semiconductor material have large direct band gap which can be further increased by reducing the size, nanocrystals or quantum dots of II-VI material can be formed by using chemical route, without much difficulty [41]. Good photo sensitivity of II-VI materials make them better candidates for application in optic and photonic device [42]. The wide band gaps of these materials make them suitable material for application as luminescent materials in the UV to visible region. ZnS is better for application as phosphor due to its better chemical stability as compared to the other chalcogenides such as ZnSe [37]. ZnS has short cathodoluminescence decay time, making it suitable for the luminescent application [41]. Exciton binding energy of for ZnS is also quite high. The high exciton binding energy supports stable high-yield luminescence and makes these materials much better candidate for applications in lasers and the excitonic-related device applications. Also as shown by the following equation, the PL intensity increases almost exponentially with increase in the binding energy [44],

$$I(T) = \frac{I_o}{1 + Ae^{(-\frac{E_a}{k_b T})}} \tag{1.16}$$

Where, I is the PL intensity, I_o is the peak intensity at 0K, E_a is the activation energy or the binding energy, K_b is the Boltzmann constant and T is the temperature.

The repeatable electrical characteristics of ZnS layer by layer device has been studied by Jafri *et al*. [45]. They observed that the current-voltage characteristics of the devices were reversible when sufficient discharge time is given prior to repeating a measurement. It is an important property for the future application of the device in electronics. The unintentional useful defects in these materials are advantageous for application in various fields like optoelectronics. Doping of these materials further increases the applications in various fields because of the improved optoelectronic properties.

PVOH is widely used surfactant for the polymer encapsulated nanocrystals. It is easily soluble in water and has excellent film forming and adhesive properties. It is non- toxic and also

has the advantage of being biocompatible. It has closely spaced uniform gaps which are distributed in the form of array. So the nanoparticles embedded in PVOH are generally of uniform size [42]. PVOH is a non corrosive material which helps to fabricate and study the electrochemical device if the samples on this matrix.

The size of the particle embedded in the PVOH can easily be controlled by varying the reaction time of temperature. We can have the solid or liquid form of the samples as required for the characterization techniques. By taking the advantage of developments in the preparation and characterization of direct band gap semiconductors in polymer matrices, the semiconductor nanocrystals have been constructed [34-35].

In the view of the above, an attempt has been made to synthesize undoped nanocrystals of ZnS embedded in polymer matrix (PVOH). We have adopted chemical route to prepare the ZnS nanocrystals. The samples prepared have been characterized by several characterization techniques. For chemical characterization of the prepared samples, we have employed optical absorption spectroscopy, photoluminescence and energy dispersive X-ray spectroscopy.

For structural characterization we have employed X-ray diffraction technique and the scanning electron microscopy.

CHAPTER 2

Synthesis

Chapter 2

Synthesis

2.1 Introduction

The synthesis of nanoparticles had started centuries ago. Gold nanoparticles and colloidal gold were used extensively in some countries for various purposes. Around thousand years ago, gold nanoparticles was used in an organic dye in china. They used it for giving red color to the ceramic porcelains. Colloidal gold has its major application in medical field, for example, for the treatment of arthritis, which still continues. In 1857, Faraday published his study on the preparation and properties of colloidal dispersion of gold and the samples prepared by him were stable for almost a century before being destroyed during world war.

The research in the field of nanometer scale world accelerated after the advent of the technologies which could see and manipulate the matter in this dimension. Modern quantum dot (Nanoparticle) technology traces its origin back to the mid 1970s.

2.2 Methods adopted to prepare nanoparticles

There are many methods to synthesize nanoparticles and also many ways to group these methods. On the basis of the approaches followed to fabricate the nanoparticles, they are grouped as top-down and bottom-up approaches, which may be again grouped broadly as chemical and physical methods.

2.2.1 Top-down approach

Top-Down approaches remove, reduce, subtract, or subdivide a bulk material to make nanoparticles. Top-Down methods, therefore, are considered to be subtractive. Top-Down fabrication methods logically resides within the realm of engineering and physics. Top-Down fabrication dominates nanotechnology today although significant ground has been gained by bottom-up methods. It can be done by following four methods,

(a) **Milling** – This method is mainly used to produce nanoparticles for use in nanocomposites and nanograined bulk materials. This method suffers from the following drawbacks.

- The nanoparticles formed by milling have a broad size, shape and geometry distribution.
- Lots of impurities from milling medium come.
- Defects are noticed in the nanoparticles produced by milling. But the preparation of nanocomposites and nanograined bulk materials require lower sintering temperature and in these materials the defects can be annealed by sintering.

(b) **Attrition** – Nanoparticles produced by this method have sizes ranging from few tens to several hundred nanometers in diameter.

(c) **Repeated thermal quenching** – This also produces nanoparticles by breaking a bulk material into small pieces, provided that the material has low thermal conductivity and large volume charge with increase in temperature. But this method is difficult to control.

(d) **Lithography** – It is the process of transferring a pattern into a reactive polymer film, termed as resist, which will subsequently be used to replicate that pattern into an underlying thin film or substrate.

Lithography is sometimes considered as hybrid approach, since the growth of thin films is Bottom-up whereas the etching is Top-down approach, while nanolithography and nanomanipulation are commonly a Bottom-up approach.

2.2.2 Bottom-up approach

Bottom-up fabrication approaches selectively combine atoms or molecules to form nanomaterials. Bottom-up fabrication methods, therefore are considered to be additive. Bottom-up fabrication methods reside within the realm of chemistry and biology.

It has two approaches, namely, thermodynamic and kinetic.

1. **Thermodynamic approach** – This method follows the following sequence to fabricate the nanoparticles.
    - Generation of super saturation
    - Nucleation
    - Subsequent growth

The steps followed, specifically for metals, non-oxide and oxide semiconductors are as follows,

(1) **Metallic nanoparticles** – By reduction of metal complexes in dilute solution thereby producing metal colloidal dispersions.

(2) **Non-oxide semiconductors** – Pyrolysis of organometallic precursors dissolved in anhydrate solvents at elevated temperature in an airless environment in the presence of polymer stabilizer or capping material.

(3) **Oxide nanoparticles** – By sol-gel processing, forced hydrolysis, controlled release of ions, vapor phase reactions and solid state phase segregation.

The above methods follow homogeneous nucleation. Following methods uses heterogeneous nucleation method

- Thermal oxidation
- Sputtering
- Argon plasma

2. **Kinetic approach** – In this method formation of nanoparticles is achieved by any one of following techniques

- By limiting the amount of precursors available for the growth as in Molecular Beam Epitaxy (MBE).
- By confirming the process in limited space. This is done by following four ways

(a) Liquid droplets in gas phase in aerosol synthesis and spray Pyrolysis.
(b) Liquid droplets in liquid as in micelle and micro emulsion synthesis.
(c) Template based synthesis
(d) Self terminating synthesis

In Top-down approach, some problems are faced like imperfection in surface structure, crystallographic damage to the processed patterns, defects due to etching. These may leads to changes in physical properties and surface chemistry, since the surface to volume ratio is very large in nanoparticles. These imperfections may again lead to reduced conductivity due to inelastic surface scattering which leads to the generation of excessive heat and thus impose extra challenge to the device design fabrication.

Bottom-up approach is comparatively better in case of nanomaterials, because in nanometer scale all the tools are too big to deal with the dimensions. Bottom-up approaches also give structure with less defects, more homogeneous composition and better short and long range ordering. In Bottom-up approach, the synthesis is mainly driven by the reduction of Gibbs free energy, so the nanomaterials produced are closer to the equilibrium state. In Top-down approach, there is internal stress in addition to defects and contamination.

2.2.3 Chemical and physical methods

These methods are also grouped broadly into chemical and physical techniques. All the above methods are mainly chemical methods except lithography. Following are the physical techniques used to synthesize the nanoparticles,

1. Lithographic techniques

- Photolithography
- Phase shifting optical lithography
- Electron beam lithography
- X-ray lithography
- Focused ion beam lithography
- Neutral atomic beam lithography
- Deep ultra-violet lithography

2. Nanomanipulation

- Scanning tunneling microscopy (STM)
- Atomic force microscopy (AFM)
- Near-field scanning electron microscopy (NSOM)
- Nanomanipulation
- Nanolithography

3. Soft lithography

- Micro-contact printing
- Molding
- Nanoimprint
- Dip-pen lithography

4. Self assembly of nanoparticles or nanowires

- Capillary forced induced assembly
- Dispersion interaction assisted assembly
- Shear force assisted assembly
- Electric field assisted assembly
- Covalently linked assembly
- Gravitational field assisted assembly
- Template assisted assembly

The main advantage of chemical method is that it is simple and less expensive. In the chemical techniques, there is a possibility of manipulation at the molecular level. Because of mixing at the molecular level, good chemical homogeneity can be achieved. Also, by understanding the relationship between how matter is assembled on an atomic and molecular level, and the material macroscopic properties, molecular synthetic chemistry can be tailor designed to prepare novel starting components. Better control of the particle size, distribution can be achieved in particle synthesis. To get benefit from the advantages of chemical processing, an understanding of the principle of crystal chemistry, thermodynamics, and phase equilibrium

and reaction kinetics is required. Chemical method is also having some problems like; in some preparation the chemistry is complex and hazardous. Entrapment of impurities in the final product are found, which needs to be avoided or minimized to obtain desired properties. For some of the systems, it may become difficult to scale up for economical production of a large quantity of material. Agglomeration is also a problem and must be avoided at any stage of the synthesis process.

2.3 Properties in the fabrication of nanoparticles

When a nanoparticle is fabricated it must have

1. Identical size (uniform size distribution)
2. Identical shape or morphology
3. Identical chemical composition
4. Identical crystal structure among different particles and within individual particle
5. Mono dispersed that means there should not be any agglomeration.

2.4 Present work

In the present investigation, Chemical methods are followed to prepare samples of ZnS. Poly-vinyl alcohol (PVOH) is used as the matrix. 5wt % solution of Poly-vinyl alcohol is taken as a matrix (capping agent). It is prepared by stirring 5 gm of PVOH in 100 ml of water at 70˚C and 300 rpm for 3hrs. Aqueous solution of $ZnCl_2$ and Na_2S are used to prepared ZnS nanocrystals. These solutions are prepared in such a way that the molecular weight ratio of the chemicals in the solution becomes 1:1. PVOH and $ZnCl_2$ solutions are then mixed in 2:1 volume ratio in magnetic stirrer at controlled temperature and rotations per minute. To the above solution Na_2S solution is added drop by drop, to make the solution completely milky. The solution is then kept overnight at room temperature for stabilization. The samples thus prepared are characterized. The reaction followed in the synthesis of ZnS nanocrystals is as follows:

$$PVOH + ZnCl_2 + Na_2S \longrightarrow PVOH + ZnS + 2NaCl$$

CHAPTER 3

Characterization

Chapter 3

Characterization

3.1 Introduction

Structural and chemical characterization techniques are adopted to obtain the important properties of nanomaterials. In the research of nanomaterials, most important thing is the availability of technology to visualize interior of the nanomaterials and to have the capability to modify and manipulate in that nanometer range. Many advanced characterization techniques are now-a-days available that have made extensive research in nanometer range possible.

3.2 Characterization Techniques

The characterization techniques can be divided into the following two categories, according to the type of information provided by the techniques.

3.2.1 Chemical characterization techniques

These techniques give internal details of the sample. It includes the following techniques

- Optical Absorption Spectroscopy (OAS)
- Energy Dispersive X-ray Spectroscopy (EDS)
- Photoluminescence (PL) Spectroscopy
- Raman Spectroscopy
- Fourier Transform Infrared Spectroscopy
- Electron Spectroscopy
- Ionic Spectrometry
- Rutherford Backscattering Spectrometry (RBS)
- Secondary Ion Mass Spectrometry (SIMS)

3.2.2 Structural characterization techniques

These Techniques give the information about the crystal structure, crystallinity, lattice constants, shape and size of the nanoparticles. Structural characterization includes the following Techniques:

- X-ray Diffraction (XRD) Study
- Scanning Electron Microscopy (SEM)
- Transmission Electron Microscopy (TEM)
- Small Angle X –Ray Scattering (SAXS)
- Scanning Probe Microscopy (SPM)
    (a) Scanning Tunneling Microscopy (STM)
    (b) Atomic Force Microscopy (AFM)

3.3 Characterization Techniques used in Present work

Following Techniques are used to characterize the samples prepared in the present investigation.

3.3.1 Optical Absorption spectroscopy (OAS)

If light is made to fall on them, most of the materials absorb some portion of it. The amount and wavelength of light absorbed depends upon the chemical and electronic structure of the absorbing material. This phenomenon is utilized in Optical Absorption spectroscopy to know the structure and properties of the sample. The absorption spectrometer records the absorption of the sample with respect to wavelength. This spectrum is then used to get various information about the material. It gives us the band gap, absorption coefficient and absorbance. Further, using these data we can get the particle size and transmittance of the material. The basic phenomena and instrumentation behind this spectroscopy is described below:

Electromagnetic radiation in the ultraviolet (200-400nm) and visible (400-800nm) region have energies between 36 to 143Kcal/mol [46]. This much of energy is sufficient to excite electrons from one molecular orbital to a higher unoccupied molecular orbital to a higher energy.

Let us suppose that the molecule is in ground state as shown in fig (3.1). If in the ground state, it receives electromagnetic radiation of wavelength corresponding to the energy difference (E2-E1), the sample absorbs radiation and the electron in the E1 level is excited to higher E2 level and the sample is said to be in the excited state. The spectrometer records the wavelength at which absorption occurs along with the degree of absorption. The lowest energy transition is most favored i.e., between the highest occupied molecular orbital (HOMO) and the lowest unoccupied molecular orbital (LOMO).

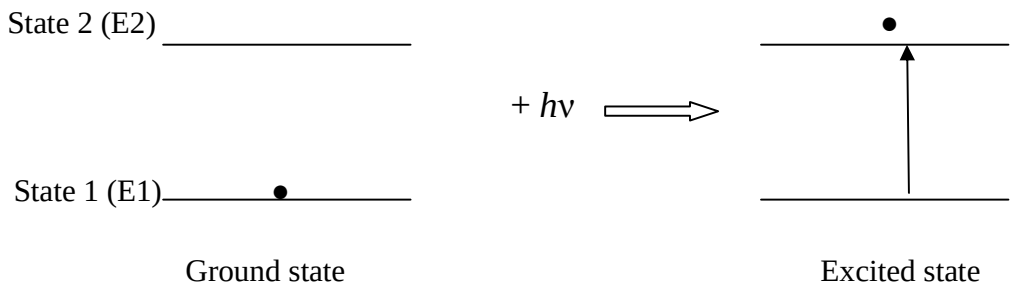

Figure 3.1 Excitation of electron after absorption of electromagnetic radiation

The optical absorption spectrometer is of two types:

- Single beam optical spectrometer
- Double beam optical spectrometer

The class depends on the fact whether the absorption of the sample and references are measured sequentially or simultaneously. The basic circuits of both the types are shown ion the fig. (3.2).

The fundamental absorption which corresponds to electron excitation from the valence band to the conduction band can be used to determine the value of the optical band gap. The relation between absorption coefficient (α) and the incident photon energy ($h\nu$), described by Tauc is used for the calculation and it is given by [32]:

$$(\alpha h\nu)^{1/n} = K(h\nu - \mathrm{E_g}) \qquad (3.1)$$

Where α can be calculated by the following relation:

$$\alpha = \frac{2.303A}{t} \tag{3.2}$$

Where α is the absorption coefficient in cm^{-1}, h is the Planck's constant, v is the frequency of the incident light, K is a constant, E_g is the band gap of the material, A is the absorbance of the material, t is the sample thickness or the length of the light path through the sample (cuvette) and the value of n depends upon the transition. It has a value of $^1/_2$ for the direct allowed transition, 2 for the indirect allowed transition, $^3/_2$ for the direct forbidden transition and 3 for the indirect forbidden transition. The value of the optical bandgap of the material is obtained by extrapolating the straight line portion of $(\alpha hv)^2$ versus hv (e.g. for direct band gap materials) plot to the (hv) axis, for α = 0, gives the value of the band gap. The band gap thus obtained is then utilized for determining the particle size using various relations. Optical absorption studies are made on a HITACHI U-3210 double beam spectrophotometer.

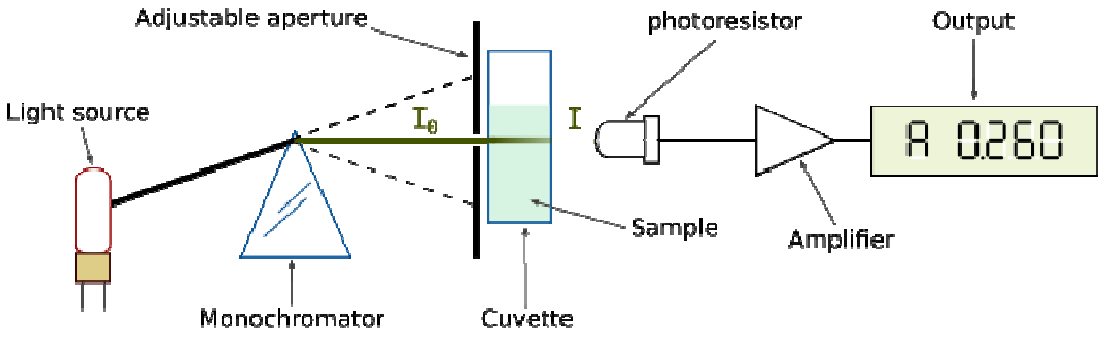

Figure 3.2 Single beam UV-visible spectrometer

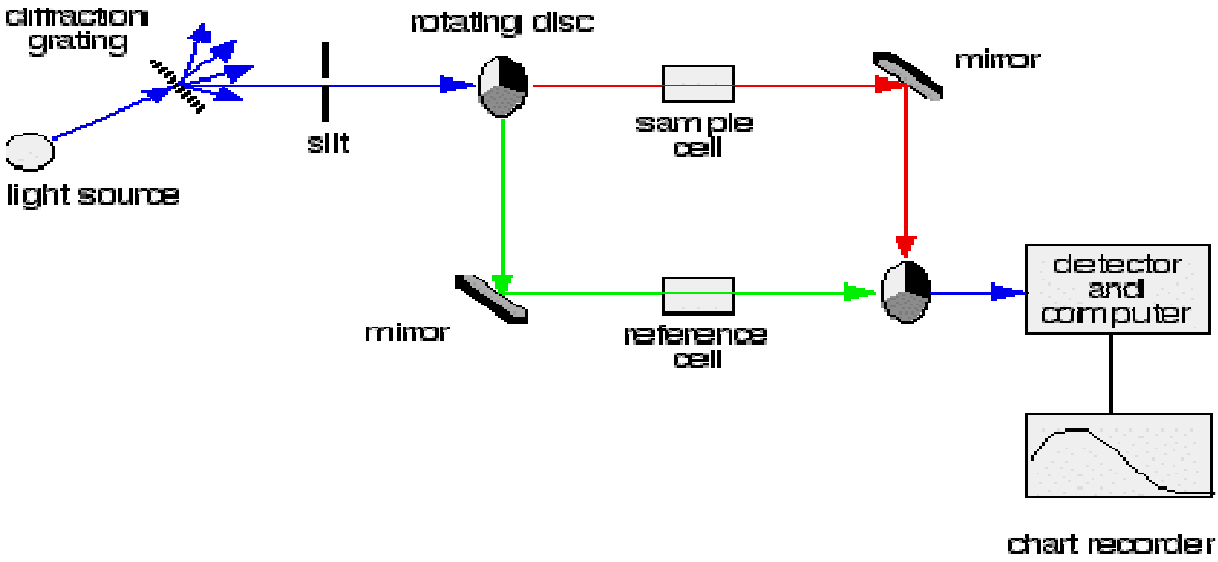

Figure 3.3 Double beam UV-visible spectrometer

3.3.2 Photoluminescence (PL) spectroscopy

All solids including semiconductors have so-called "energy gap" for the conducting electrons. In order to understand the concept of a gap in energy, first consider that some of the electrons in a solid are not firmly attached to the atoms, as they are for single atoms, but can hop from one atom to another. These loosely attached electrons are bound in the solid by differing amounts and thus have much different energy. Electrons having energies above a certain value are referred to as conduction electrons, while electrons having energies below a certain value are referred to as valence electrons. This is shown in the diagram where they are labeled as conduction and valence bands. The word band is used because the electrons have a multiplicity of energies in either band. Furthermore, there is an energy gap between the conduction and valence electron states. Under normal conditions electrons are forbidden to have energies between the valence and conduction bands. If a light particle (photon) has energy greater than the band gap energy, then it can be absorbed and thereby raise an electron from the valence band up to the conduction band across the forbidden energy gap (See diagram.). In this process of photo excitation, the electron generally has excess energy which it loses before coming to rest at the

lowest energy in the conduction band. At this point the electron eventually falls back down to the valence band. As it falls down, the energy it loses is converted back into a luminescent photon which is emitted from the material. Thus the energy of the emitted photon is a direct measure of the band gap energy, Eg. The process of photon excitation followed by photon emission is called photoluminescence.

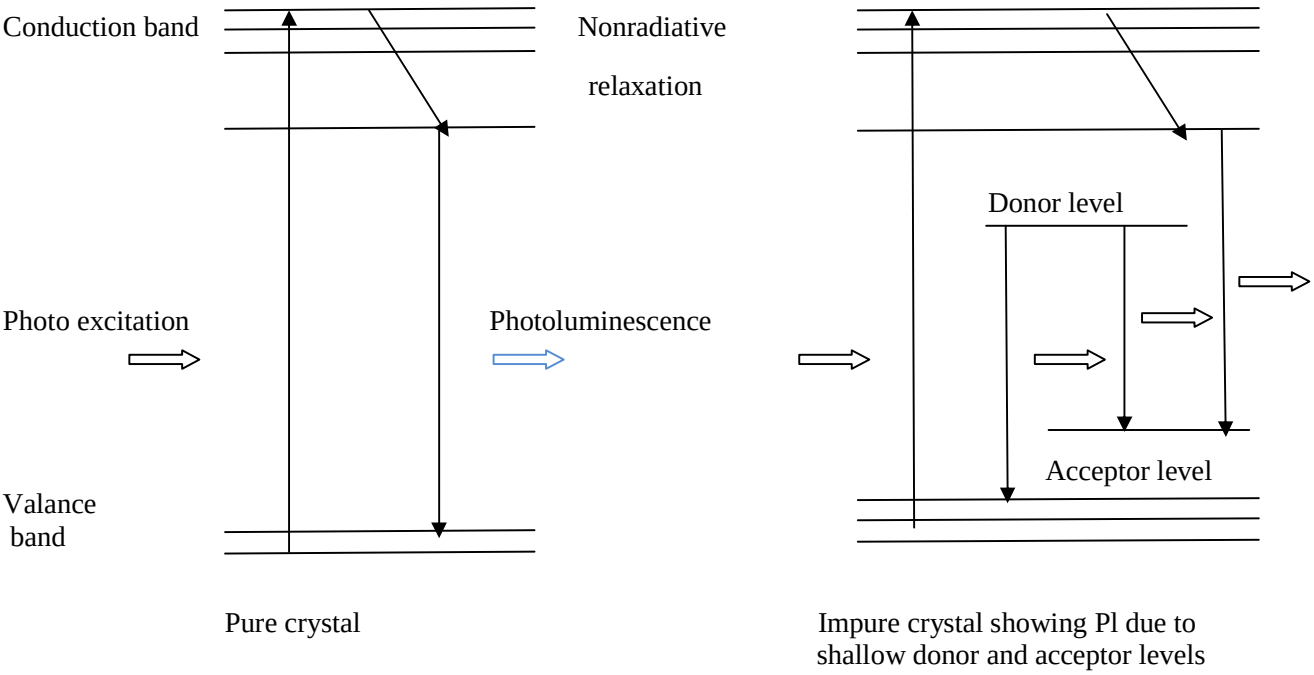

Figure 3.4 Photoluminescence

In pure samples, an electron-hole pair, called an exciton can move between these two carriers with a small binding energy. The energy of the emitted photon from a band-to-band transition, an exciton recombination, or any of a number of other possible transitions is then characteristic of the energy levels involved [39]. In doped samples, relative recombination can also occurs via shallow donor or acceptor levels. Three possible transitions are donor level to valence band, conduction band to acceptor level and donor to acceptor (Fig 3.4). These peaks will appear at the low energy side of the exitonic transitions in PL measurements, a sample is irradiated with a visible light source, which stimulates the material to an excited electronic state. In this process of photo excitation of electrons from their ground state in the valence band to the upper state of the

conduction band, the electrons generally have excess energy which they loses through non-radiative relaxation before coming to rest at lowest energy in the conduction band. At this point the electrons have a probability of radiatively recombining with holes in the valence band. The photoluminescence is recorded with HITACHI F-2500 fluorescence spectrophotometer.

3.3.3 X-Ray Diffraction

X-ray is a form of electromagnetic radiation which has a wavelength in the range of 10 to 0.01 nanometers, corresponding to frequencies in the range 30 petahertz to 30 exahertz. Each crystalline solid has its unique characteristic X-ray powder pattern which is used as the "fingerprint" for its identification. Once the material has been identified, X-ray crystallography may be used to determine its structure, interatomic distance, unit cell dimension etc. As wavelength of X –rays is about the same as size of an atom, they are ideally suited to probe crystalline structure at the atomic level.

A typical diffractometer consists of a source of radiation, a monochromator to choose the wavelength, slits to adjust the shape of the beam, a sample and a detector. When a monochromatic X-ray beam with a wavelength $\boldsymbol{\lambda}$ is projected onto a material at an angle θ, diffraction occurs from different atoms. Diffracted waves from these atoms can interfere with each other and the resultant intensity distribution is strongly influenced by this interference. If the atoms are arranged in a periodic fashion, as in crystals, the diffracted waves will consist of sharp interference peaks as in the distribution of atoms. The X-ray radiation most commonly used is that emitted by copper, whose characteristic wavelength for the K radiation is 1.5418 A. when the incident beams strikes a sample, diffraction occurs in every possible orientation of 2θ. The diffracted beam may be detected by using a movable detector which is connected to a chart recorder. Basically counter is set to scan over a range of 2θ values at a constant angular velocity. In general, a 2θ range of 5 to 80 degrees is sufficient to cover the most useful part of the powder pattern. The scanning speed of the counter is usually 2θ of 2degrees/min and therefore, about 30 minutes are needed to obtain a trace. X- Ray diffraction: X-ray diffraction is recorded on Pro X-ray diffractometer, using CuK_{α} radiation ($\lambda = 0.15406$ nm).

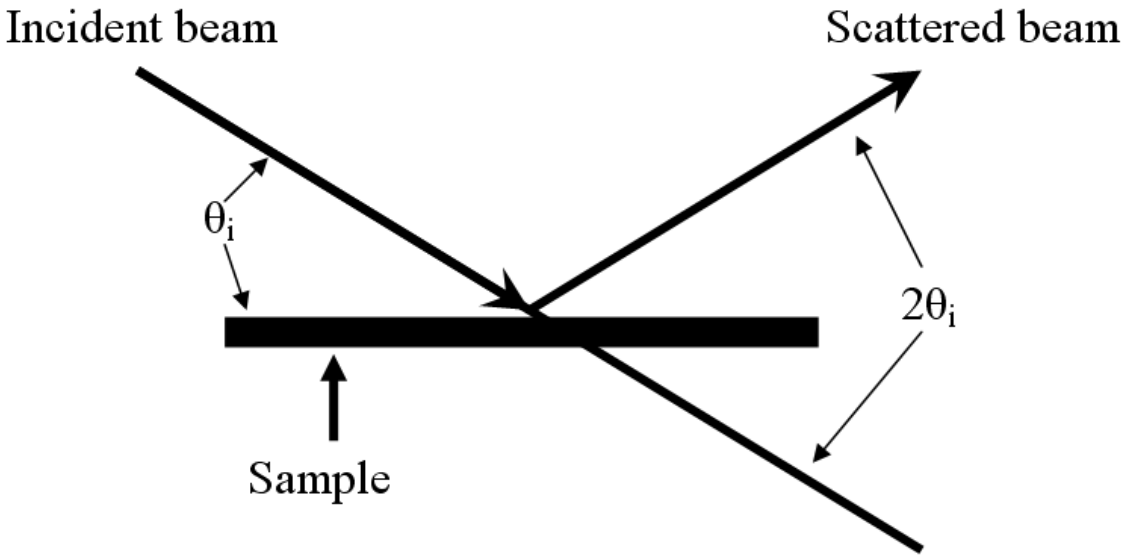

Only planes of atoms that share this normal will be seen in the θ - 2θ Scan

Figure 3.5 θ - 2θ Scan

In 1913, Bragg predicted a simplest explanation for the observed diffraction pattern that result from the passage of X-rays through a crystal. According to him Constructive interference occurs only for certain θ's correlating to a (*hkl*) plane, specifically when the path difference is equal to n wavelengths [43]. Thus when this law is satisfied, it produces a consecutive interference among the diffracted waves. It is given by

$$n\lambda = 2\, d \sin\theta \qquad (3.3)$$

Where *n* is an integer representing the order of the peak, λ is the characteristic X-ray wavelength (in angstrom), *d* is interatomic spacing (in angstrom) and θ is the angle of diffraction (in degrees).

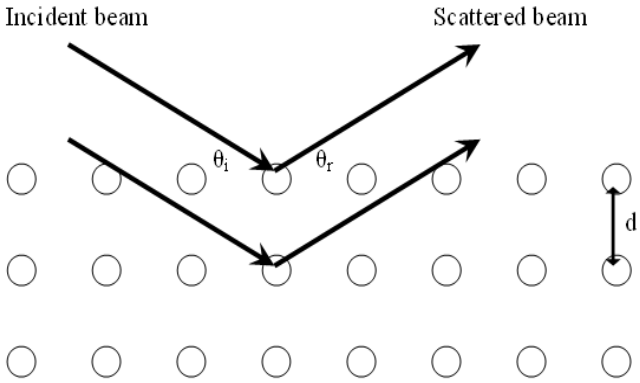

Figure 3.6 Bragg's Law

By varying the angle θ, the Bragg's law conditions are satisfied by different d-spacing in polycrystalline materials. Plotting the angular positions and intensities of the resultant diffracted peaks of radiation produces a pattern, which is characteristic of the sample. Where a mixture of different phase is present, the resultant diffractogram is formed by addition of individual patterns. The above diffraction condition can be written in vector form

$$2k \cdot G + G^2 = 0, \tag{3.4}$$

Where

k is the incident wave vector

k' is the reflected wave vector

G is a reciprocal lattice vector such that

$$G = \Delta k = k - k' \tag{3.5}$$

Diffraction peaks are accurately measured with XRD, which makes it the best method for characterizing homogeneous and inhomogeneous strains. Homogeneous or uniform elastic strain shifts the diffracted peak positions. From the shift in peak positions, one can calculate the change in d-spacing, which is the result of the change of lattice constant under strains. Inhomogeneous strains vary from crystallite to crystallite or within a single crystallite and these causes a broadening of the diffraction peaks that increases with sin θ. Peak broadening is also caused by the finite size of crystallites, but here the broadening is independent of sin θ. When both crystallite size and inhomogeneous strains contribute to peak width, these can be separately

determined by careful analysis of peak shapes. If there is no homogeneous strains, the crystallite size *D*, can be estimated from the peak width with the Debye Scherer's formula given by [47],

$$D = \frac{K\lambda}{\beta cos\theta} \tag{3.5}$$

Where *K* is the Scherer's constant, having a value of 0.9, λ is the X-ray wavelength, β is the full width at half maximum (FWHM) of diffraction peak (in radians) and θ is the Bragg's diffraction angle in degrees.

Scherer's relation works only if stress-related and instrument-related broadening is negligible in comparison to particle size effects. This condition is often met with particle size below 100 nm and this technique is very useful to determine particle size in nanometer range. The information on lattice strain on the particles after applying the correction for instrument broadening can be obtained from the following relation between strain and particle size given by [48],

$$\frac{\beta cos\theta}{\lambda} = \frac{1}{D} + \frac{\eta sin\theta}{\lambda} \tag{3.6}$$

Where η, is the effective strain. The slope of the plot between $\beta cos\theta/\lambda$ and $\eta sin\theta/\lambda$ gives the value of strain. The inverse of y-axis intercept obtained by extrapolation of the same plot gives the average particle size.

3.3.4 Scanning electron microscope (SEM)

SEM is an electron microscopy technique. The image in an SEM is produced by scanning the sample with a focused electron beam and detecting the secondary or backscattered electrons. The resolution of the SEM approaches a few nanometers, and the instruments can operate at magnifications that are easily adjusted from 10 to over 1, 00,000. SEM produces topographical information like optical microscope as well as it also provides chemical composition information near the surface.

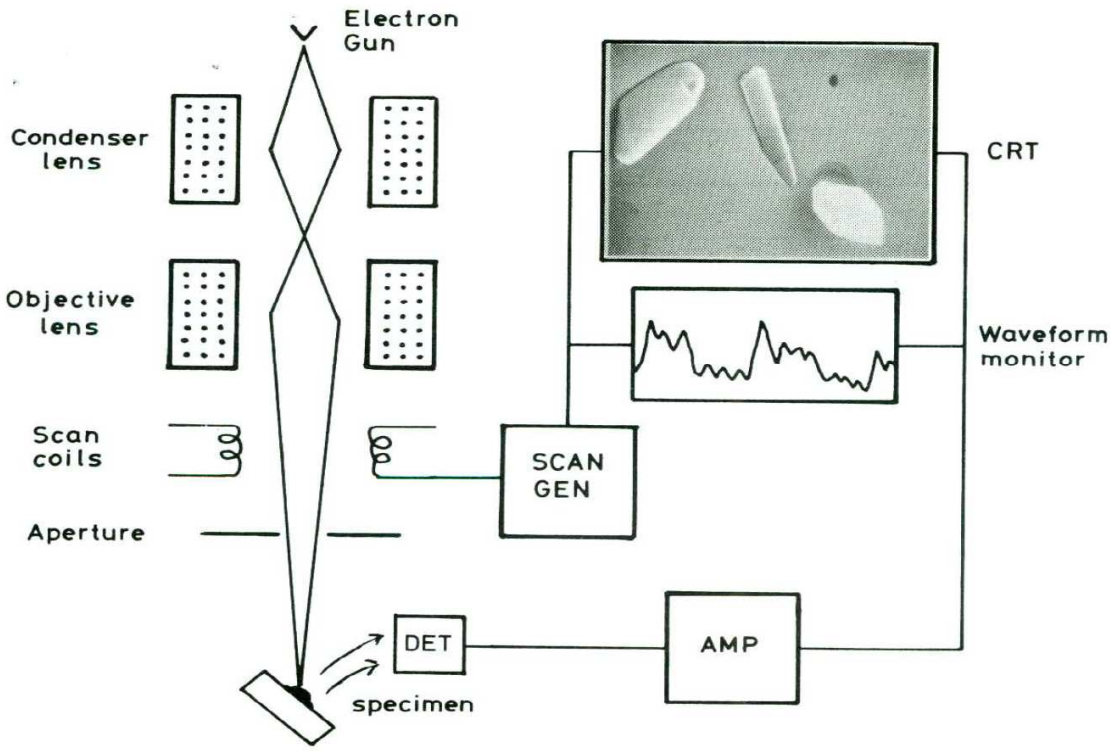

Figure 3.7 Scanning Electron Microscope

In a typical SEM we have a source (electron gun) of the electron beam which is accelerated down the column; a series of lenses (condenser and objective) which act to control the diameter of the beam as well as to focus the beam on the specimen; a series of apertures through which the beam passes and which affect properties of that beam; controls for specimen positions (x, y, z- height) and orientation (tilt, rotation); an area of beam that generates the several types of signals that can be detected and processed to produce an image or spectra. The whole setup is maintained at high vacuum level.

When the beam of electrons strikes the surface of the specimen and interacts with the atoms of the sample, signals in the form of secondary electrons, back scattered electrons and characteristic X-rays are generated that contain information about the sample's surface topography, composition, etc. The SEM can produce very high-resolution images of a sample surface, revealing details about 1-5 nm in size in its primary detection mode i.e. secondary electron imaging. Characteristic X-rays are the second most common imaging mode for an SEM. These characteristic X-rays are used to identify the elemental composition of the sample by a

technique known as energy dispersive X- ray (EDX). When a high energy primary electron interacts with the atom, it undergoes either inelastic scattering with atomic electrons or elastic scattering with atomic nucleus. In an inelastic collision the primary electron, transfer part of its energy to the other electron. When the energy transfer is large enough the other electron will emitted from the surface of the sample. If the emitted electron has energy less than 50eV, it is known a secondary electron. Backscattered electrons are the high energy electron that are elastically scattered and essentially possess the same energy as the primary electrons. The probability of backscattering increases with the atomic number of the sample material. Back-scattered electrons (BSE) that come from the sample may also be used to form an image. BSE images are often used in analytical SEM along with the spectra made from the characteristic X-rays as clues to the elemental composition of the sample. In a typical SEM, the beam passes through pairs of scanning coils or pairs of deflector plates in the electron column to the final lens, which deflect the beam horizontally and vertically so that it scans in a raster fashion over a rectangular area of the sample surface. Electronic devices are used to detect and amplify the signals and display them as an image on a cathode ray tube in which the raster scanning is synchronized with that of the microscope. The image displayed is therefore a distribution map of the intensity of the signal being emitted from the scanned area of the specimen. SEM requires that the specimens should be conductive for the electron beam to scan the surface and that the electrons have a path to ground for conventional imaging. Non-conductive solid specimens are generally coated with a layer of conductive material by low vacuum sputter coating or high vacuum evaporation. This is done to prevent the accumulation of static electric charge on the specimen during electron irradiation [49]. Data is recorded on HITACHI S 750 and ZEISS SEM analyzer.

3.3.5 Energy Dispersive X-ray Spectroscopy (EDS)

Energy dispersive X-ray analysis is a technique to analyze near surface elements and estimate their proportion at different position, thus giving an overall mapping of the sample. This technique is used in conjunction with SEM. An electron beam strikes the surface of a conducting sample. The energy of the beam is typically in the range 10-20keV. This causes X-rays to be emitted from the material. The energy of the X-rays emitted depends on the material under examination. By moving the electron beam across the material an image of each element in the

sample can be obtained. When an incident electron or photon such as X-ray, strikes an unexcited atom, an electron from the inner shell is ejected and leaves a hole or electron vacancy in the inner shell (). An electron from an outer shell fills the hole by lowering the energy, and simultaneously the excess energy is released through the emission of an X-ray. If incident photons are used for excitation, the resulting characteristic X-rays are known as fluorescent X-rays. Since each atom in the periodic table has a unique electronic structure with a unique set of energy levels, X-ray spectral lines are characteristic of the element studied. By measuring the energy of the X-rays emitted by a material, its chemical composition can be determined. The output of an EDS analysis is an EDS spectrum which is just a plot of how frequently an X-ray is received for each energy level. An EDS spectrum normally displays peaks corresponding to the energy levels for which the most X-rays had been received. Each of these peaks is unique to an atom, and therefore corresponds to a single element. The higher a peak in the spectrum, the more concentrated the element is in the specimen.

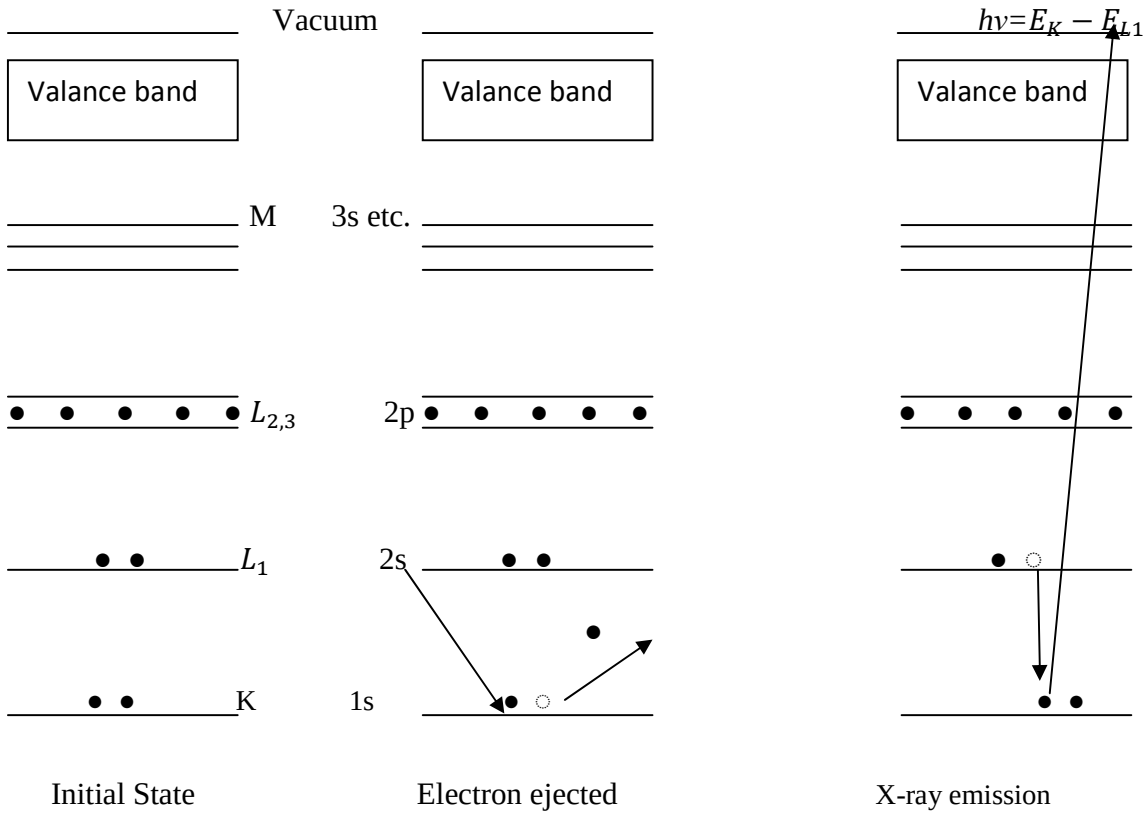

Figure 3.8 Electron energy transitions in EDS analysis

CHAPTER 4

Data analysis & Results

Chapter 4

Data Analysis & Results

Following characterization techniques have been used for characterization of fabricated ZnS samples;-

1) Optical Absorption Spectroscopy (OAS)
2) Photoluminiscence (PL) Spectroscopy
3) Energy Dispersive X-ray Spectroscopy (EDS)
4) X-ray Diffraction (XRD)
5) Scanning Electron Microscopy (SEM)

4.1 Results obtained from chemical characterization

(a) Optical Absorption Spectroscopy

The UV-visible spectra for ZnS samples 1,2,3 and 4 is given in figure 4.1, 4.2, 4.3, and 4.4 respectively. Band gaps from these curves are determined by following the procedure of Tauc [32].

From UV-visible spectra of ZnS samples, it is observed that the band gap lies in between 3.72 to 4.31 (table 4.1). this is larger than the band gap of bulk ZnS (3.68). Hence there is an obvious blue shift in all the samples, which is evidence for the effect of quantum confinement in nanoparticles. Furthermore for samples 1 and 2 we are getting excitonic peaks around 309 and 308 nm respectively. The presence of these near sharp excitonic peaks manifests the monodispersity of the ZnS samples [50]. While the absence of these prominent sharp excitonic peaks in case of samples 3 and 4 indicates the broad size distribution of particles in these samples. Also for samples 1 and 2 , we have a sholder around 248 and 243nm respectively., in addition to the main excitonic peak. These shoulders corresponds to narrow excitonic bands. Similar peaks are also observed by other workers. Chakraborty *et al.* [27] obtained the shoulder

at 202-261 nm for ZnS nanoparticles prepared in polymer surfactant gel matrix, while Kovtyukhova *et al.* [27] reported two absorption peaks at 250nm and 300 nm for ZnS nanoparticles prepared in Si film by sol-gel method. R. Bhadra *et al.* [51] also obtaind shoulder at 250 and 227 nm for ZnS nanoparticles embedded in PVOH matrix..

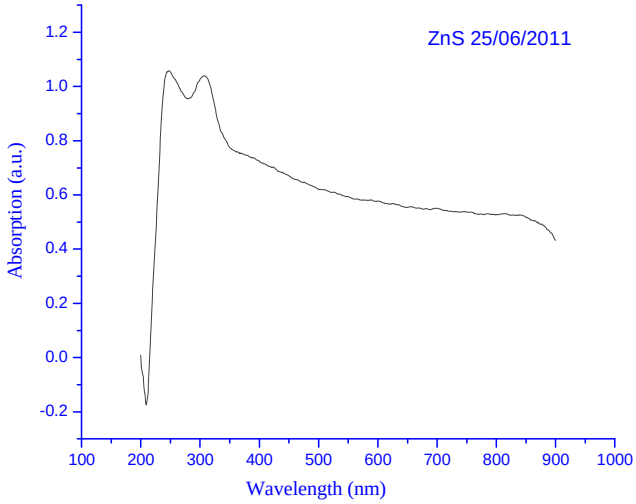

Figure 4.1 absorption spectra for sample 1

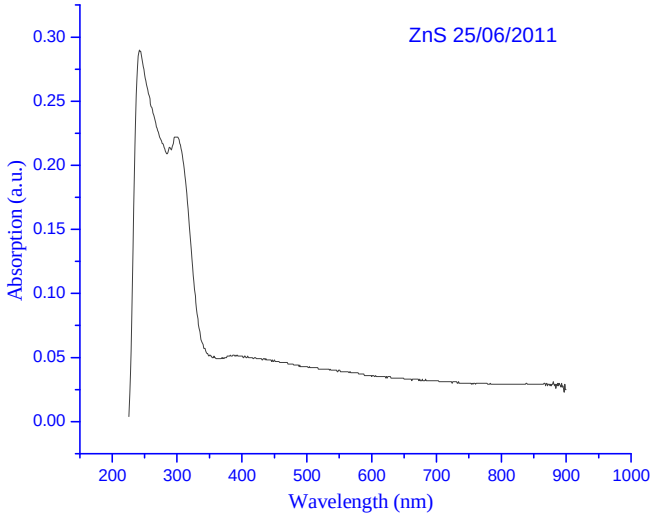

Figure 4.2 absorption spectra for sample 2

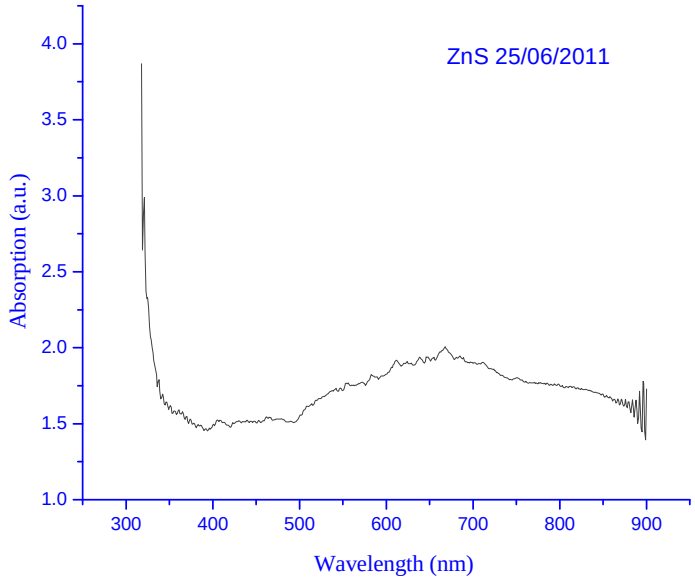

Figure 4.3 absorption spectra for sample 3

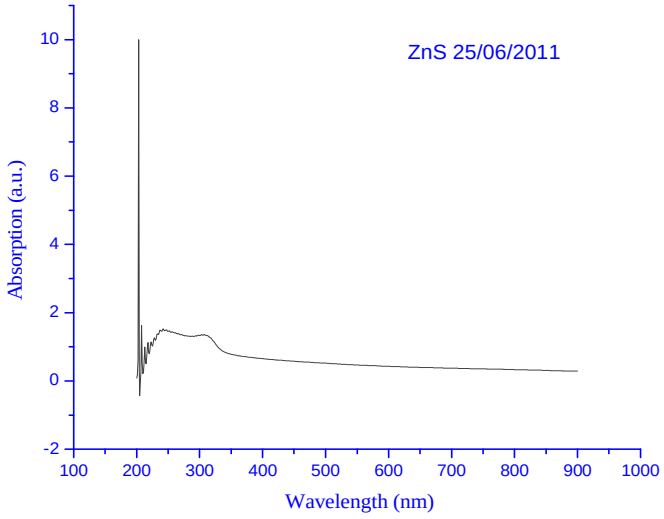

Figure 4.4 absorption spectra for sample 4

Using the band gaps obtained , the average particle size is obtained from the following models [48],

- Effective mass approximation
- Empirical pseudo-potential method
- Hyperbolic band model
- Nosaka effective mass approximation

The size estimated from EMA is taken to be the approximate size for the fabricated samples from UV-visible absorption, because EMA and HBM data almost coincides and both vary monotonically with band gap. But no such regular dependence of size have not been observed in case of data obtained by EPM and NEMA. Data given in table 4.1 indicates gradual decrease of height with increase in the band gap and almost linear relationship between height and size of nanoparticle.

Table 4.1 Band gap, size and height of ZnS samples

Sample no	Band gap	Size from EMA (nm)	Size from HBM (nm)	Size from EPM (nm)	Size from NEMA (nm)	Particle height (nm)
1.	3.76	8.06	8.052	3.99	3.99	4.46
2.	4.25	3.49	3.42	2.04	2.04	2.38
3.	3.88	7.12	7.08	3.98	3.98	4.14
4.	3.85	6.56	6.53	3.16	3.16	3.92

(b) Photoluminiscence (PL) Spectroscopy

The photoluminiscence spectra for fabricated ZnS samples 1,2,3 and 4 embedded in PVOH is given in figures 4.1, 4.2, 4.3 and 4.4 respectively. The excitations and emission

energies are given in table 4.3. all the samples are excited at energies greater than 4ev. From the photoluminiscence curve of ZnS nanoparticles embedded in PVOH matrix, we observe that the samples are luminiscent in the range 2.88ev to 3.64ev (table 4.3). Broad emission band is obtained in almost all the samples. It may be because of interaction of nanocrystals with the polymer[35, 48].

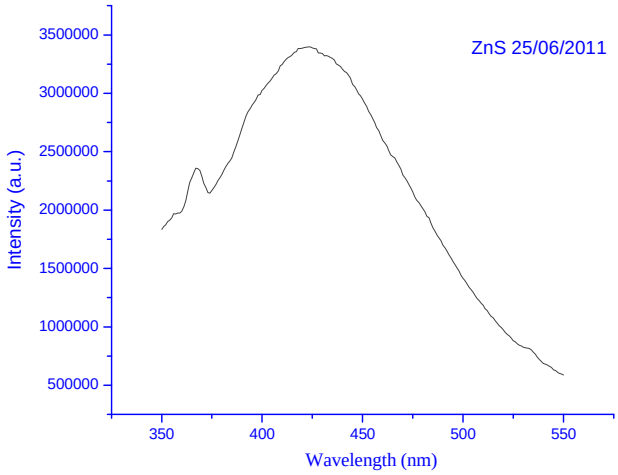

Figure 4.5 PL spectra for sample 1

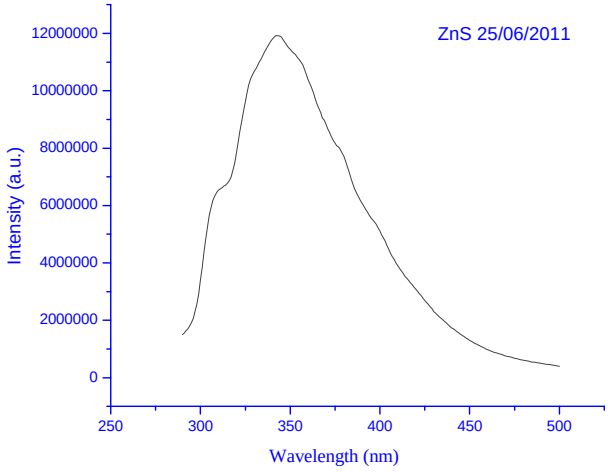

Figure 4.6 PL spectra for sample 2

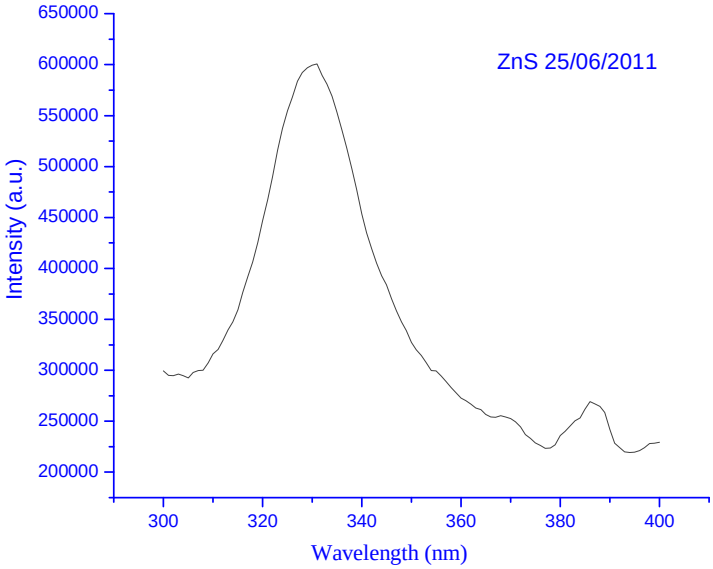

Figure 4.7 PL spectra for sample 3

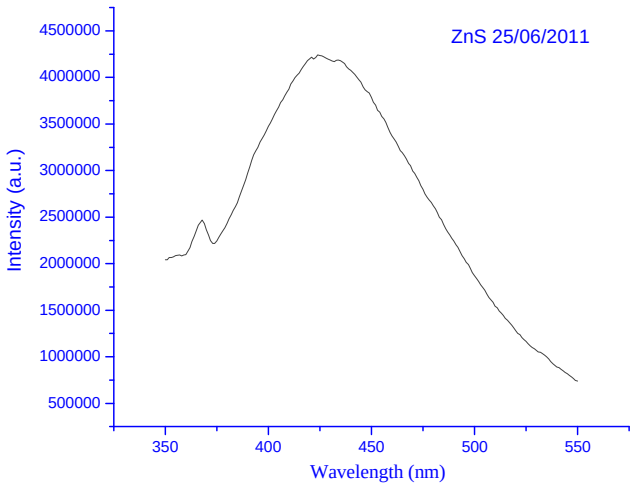

Figure 4.8 PL spectra for sample 4

The emission at the higher energy region (~ 3.6ev), which is slightly red shifted compared to the bulk band gap of ZnS (3.68), can be attributed to the band gap luminescence. The peak around 414nm is obtained in samples 1 and 4, which is the typical luminescence of ZnS (classically termed as self activated luminescence) and occurs due to trapped state emission arising from the bulk defects such as vacancies [21, 48, 52]. The sulphur vacancy in the samples is also confirmed from the EDS measurements. The observation also confirms that the relative energy position of sulphur vacancy with respect to the valence band remain unaltered whereas the position of valance and conduction band may change with change in particle size.

The observation of these selectively excited luminescence spectra depends mainly on the size distribution of nanocrystals [53]. If the size distribution is very broad, a large no of particles of different size will always be excited, resulting in a broad PL spectrum with no distinct features and independent of excitation energy. But if the distribution is extremely narrow, the emission peak will always occurs at the same energy determined by the unique crystallite size. In the intermediate case of distribution which is not too broad not too narrow, appropriate excitation energy can excite several nanoparticles simultaneously producing a PL spectrum which contains more than one peak. The photoluminescence is recorded with HITACHI F-2500 fluorescence spectrophotometer.

Table 4.2 Excitation and Emission Energy of ZnS samples along with FWHM

Sample no	Excitation Energy (eV)	Emission Energy (eV)	FWHM (eV)
1.	4.96	3.55	0.64
2.	4.13	3.37	0.97
3.	4.13	3.58	0.36
4.	4.27	3.64	0.48

The full-width-at-half-maximum (FWHM) of luminescence peaks have been estimated and presented in table 4.2. Sample 2 have the highest FWHM and sample 3 have lowest. The samples with high FWHM typically more than 50nm are considered as poor luminescent applications (such as LED).

(c) Energy Dispersive X-ray Spectroscopy (EDS)

EDS chemical characterization curves for ZnS samples, are shown in Figure, respectively. The spectra confirm the composition of ZnS particles. In addition to Zn and S some other elements are also present. Among them, C and Cu results from the grid whereas Si results from the detector. Au is present in the spectrum of sample S_1 due to gold coating.

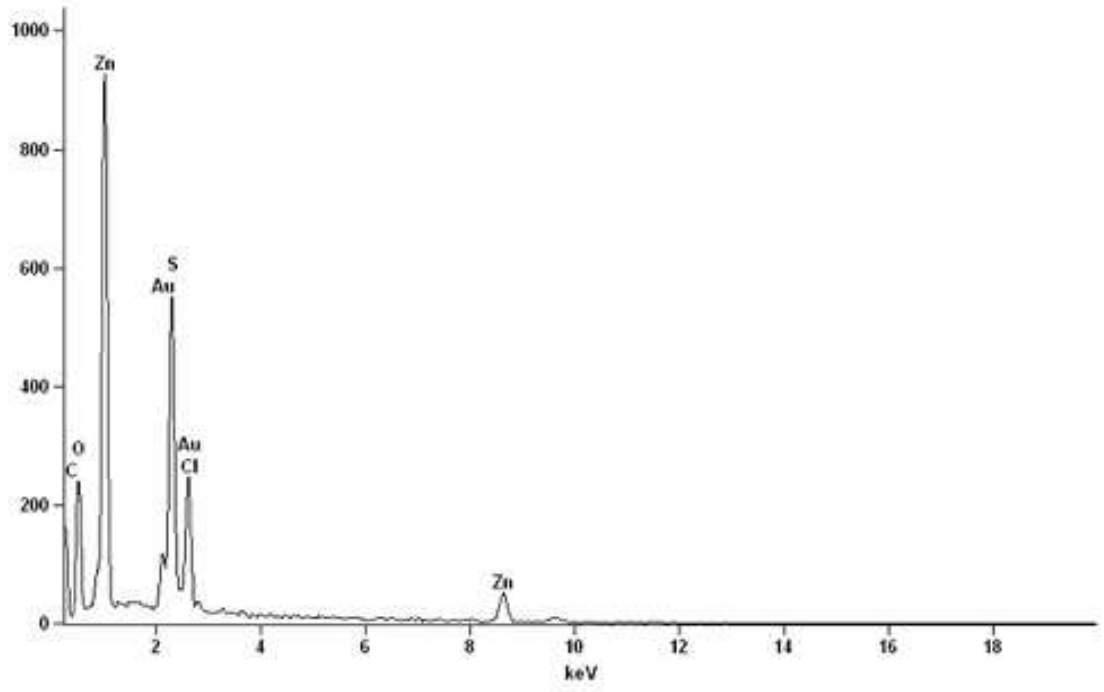

Figure 4.9 EDS pattern for sample 1

Table 4.3 Composition of Zn in different sample from EDS

Sample No	Weight % of Zn	Atomic % of Zn
1	36.80	19.61
2	14.29	3.54
3	20.68	5.80
4	33.28	12.37

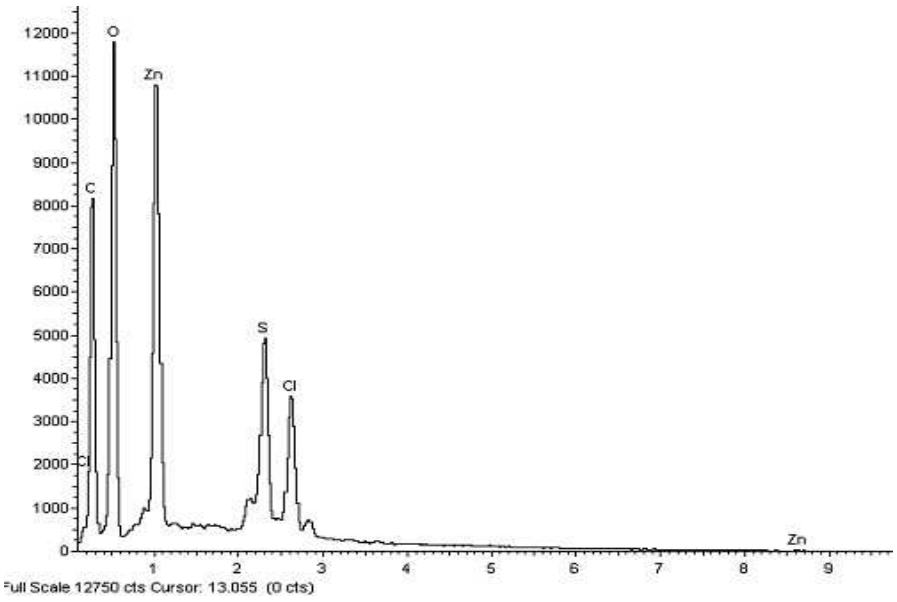

Figure 4.10 EDS pattern for sample 2

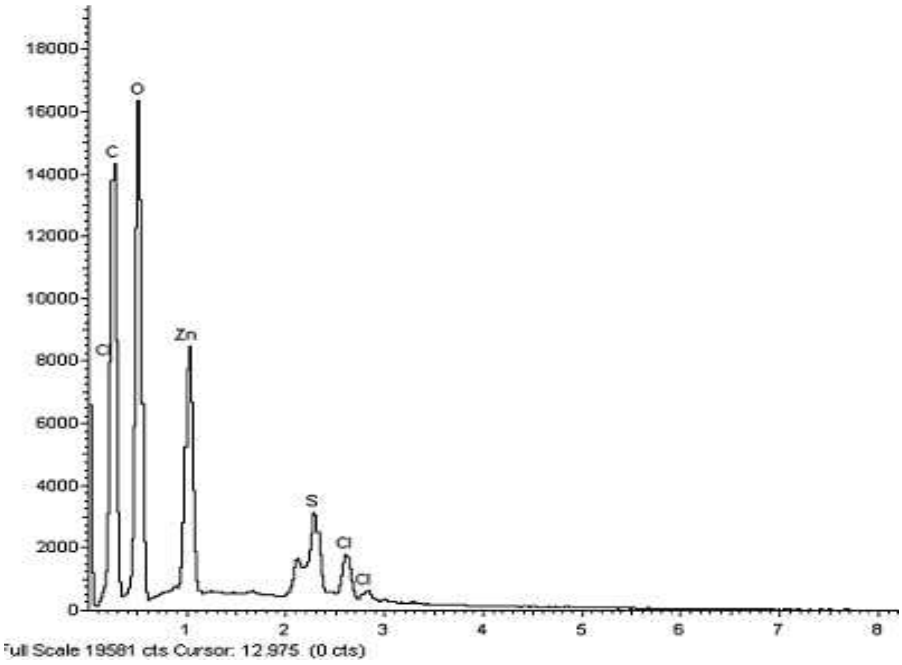

Figure 4.11 EDS pattern for sample 3

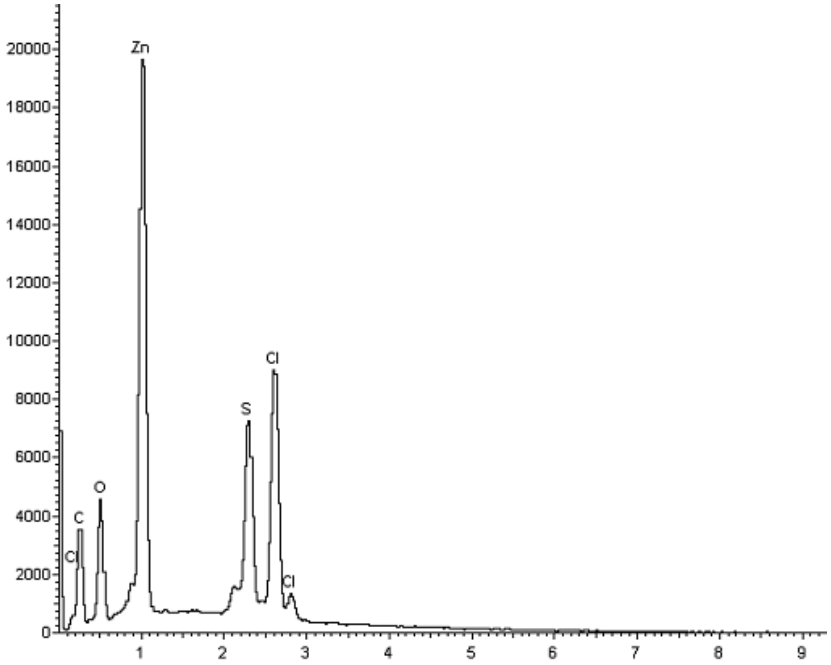

Figure 4.12 EDS pattern for sample

4.2 Results from physical characterization

(a) X-Ray Diffraction (XRD)

XRD pattern for ZnS nanocrystals embedded in PVOH matrix, taken at room temperature are shown in figures. The X-Ray pattern of the samples shows a broadening of peaks, which indicates the decreament in the size of the particles in the sample. To detect the peak positions due to matrix we have taken the XRD of the matrix deposited over a glass slide. In all samples the first broad peak at $2\vartheta = 19.5$ degrees, is due to the matrix. The other diffraction peaks (table 4.4) shows the material to be ZnS and preferred structure to be hexagonal (wurtzite) according to the standard JCPDS card. Slight shift in the some peaks from standard position is due to residual stress. The size has been calculated from half widths at full maximum of the diffraction peaks using Debye Scherrer formula [47]. From each sample size is calculated for at least three peaks except sample 2 and average value is taken (table 4.5). Size estimation from XRD results support nanodimensions and indicate confinement to be strong. A comparison of size estimated from UV-visible and XRD reveals that both characterization techniques confirm nano formation.

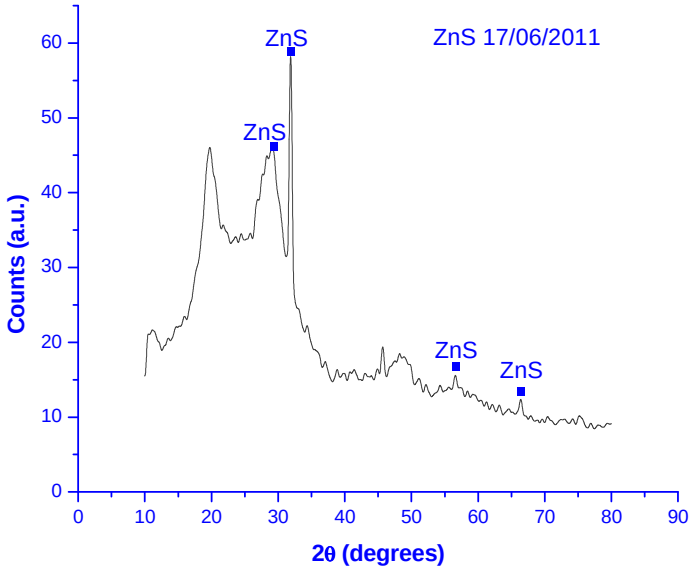

Figure 4.13 XRD spectrum for sample 1

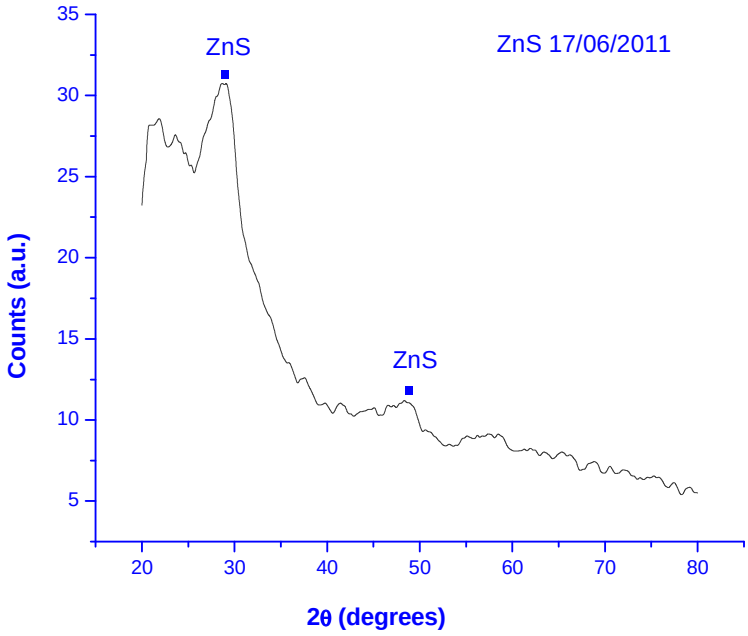

Figure 4.14 XRD spectrum for sample 2

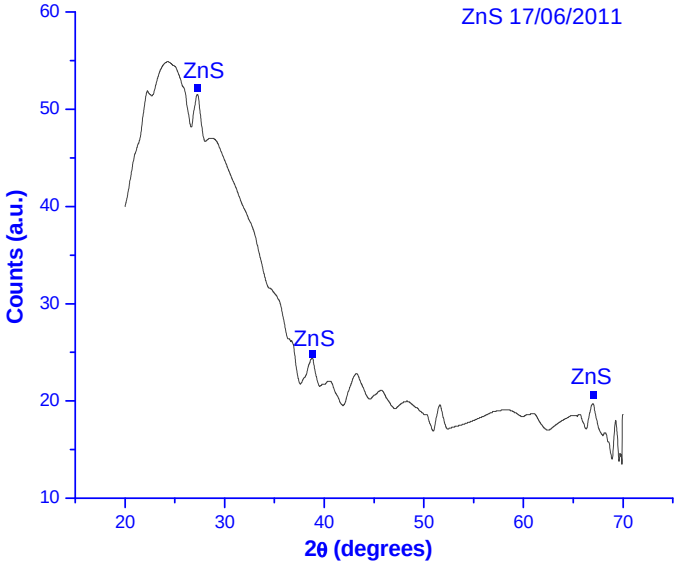

Figure 4.15 XRD spectrum for sample 3

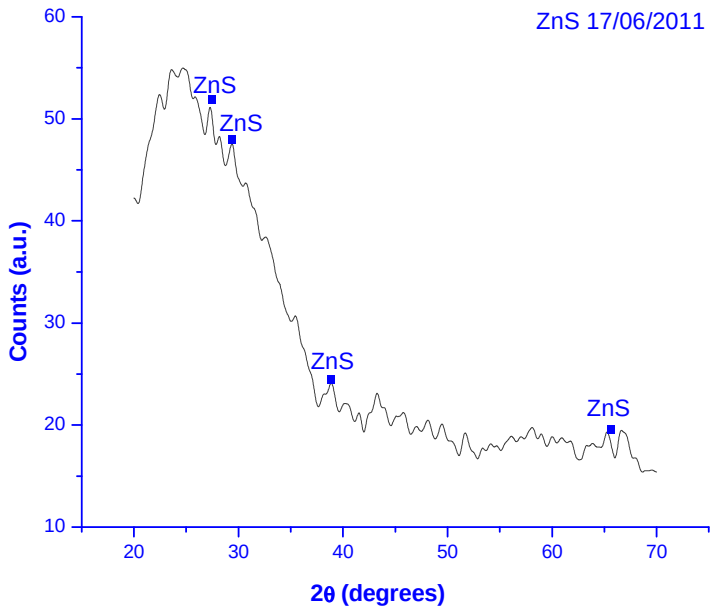

Figure 4.16 XRD spectrum for sample 4

Table 4.4 Size for ZnS samples obtained from XRD patterns

Sample no	Size in nm
1	5.78
2	2.70
3	5.68
4	6.72

Table 4.5 Various parameters for ZnS samples obtained from XRD patterns

Sample no.	*2θ = 19.5* degree	FWHM (radian)	*d*-spacing		*(hkl)*
			XRD	JCPDS	
1.	29.43	.084	3.043	3.139	(002)
	31.86	.018	2.826	2.936	(101)
	46.24	.020	1.853	1.918	(110)
2.	28.81	.077	3.162	3.139	(002)
	48.42	.060	1.735	1.918	(110)
3.	27.39	.021	3.286	3.322	(100)
	38.94	.036	2.312	2.281	(102)
	67.06	.031	1.382	1.418	(104)
4.	27.54	.021	3.198	3.139	(002)
	29.58	.023	3.173	3.139	(002)
	38.95	.033	2.299	2.283	(102)
	58.19	.021	1.591	1.606	(201)
	65.29	.024	1.254	1.481	(104)

CHAPTER 5

Application

Chapter 5

Application

5.1 Introduction

Nanometer materials have been attracting strong attention due to their interesting structure and properties. Many important potential applications have been demonstrated for nanometer material based on their unique properties. This application is based on memory application of resistive-switching devices using nanomaterials as the active components. Though the mechanism for the electrical switches has been in argument, it is generally believed that the resistive switches are related to charge storage on the nanoparticles. The resistive switches are due to electromechanical behavior of the materials. These nanoelectromechanical devices can be used as fast-response and high-density memory devices as well.

Comparing with traditional flash memories that contain the continuous silicon floating gate, the devices with the nanoparticle floating gate have advantage of high density and long retention time. Recently, resistive switches were observed on a two terminal electronic devices with metal or semiconductor nanoparticles as one of the active materials [54]. These devices can be electrically switched between two states with significant different resistances for numerous time and have good stability in both states. These two terminal devices have fast response to the external electric field and can have extremely high density due to the nanometer size of the active material. Thus they can potentially solve all technical difficulties in the three leading memory devices: dynamic random access memories (DRAM), hard disk drives (HDDs) and flash memories [55].

Nanoparticles devices are promising to be the next generation memory devices; because the electronic structure and properties of nanoparticles can be manipulated by controlling their shape and size, and nanoparticles can be soluble in solvents. The devices can be fabricated through several of chemical techniques, which can significantly lower the fabrication cost. In addition, these memory devices utilize the charge storage on nanoparticles. Due to this these devices can have high flexibility, rendering them highly compatible with other flexible electronic

devices that are regarded as next generation electronic devices. One example is the combination of resistive-memory switching device with light-emitting diode, which can be used in electronic books [54].

5.2 Memristor

In general there are six different mathematical relations connecting pairs of the four fundamental circuit variables: electric current i, voltage v, charge q and magnetic flux Q. One of these relations (the charge is the time integral of the current) is determined from the definitions of two of the variables, and another (the flux is the time integral of the electromotive force, or voltage) is determined from Faraday's law of induction. Thus, there should be four basic circuit elements described by the remaining relations between the variables (Fig. 1). The 'missing' element—the memristor, with memristance M provides a functional relation between charge and flux [56].

In the case of linear elements, in which M is a constant, memristance is identical to resistance and, thus, is of no special interest. However, if M is itself a function of q, yielding a nonlinear circuit element, then the situation is more interesting. The i–v characteristic of such a nonlinear relation between q and Q for a sinusoidal input is generally a frequency-dependent, and no combination of nonlinear resistive, capacitive and inductive components can duplicate the circuit properties of a nonlinear memristor (although including active circuit elements such as amplifiers can do so). Because most valuable circuit functions are attributable to nonlinear device characteristics, memristors compatible with integrated circuits could provide new circuit functions such as electronic resistance switching at extremely high two-terminal device densities.

The memristor is essentially a two-terminal variable resistor, with resistance dependent on the amount of charge *q* that has passed between the terminals [57].

$$V = I \cdot M(q) \tag{5.1}$$

To relate the memristor to the resistor, capacitor, and inductor, it is helpful to isolate term M (q), which characterizes the device, and writes it as a differential equation:

$$M = d\Phi_m / dQ \qquad (5.2)$$

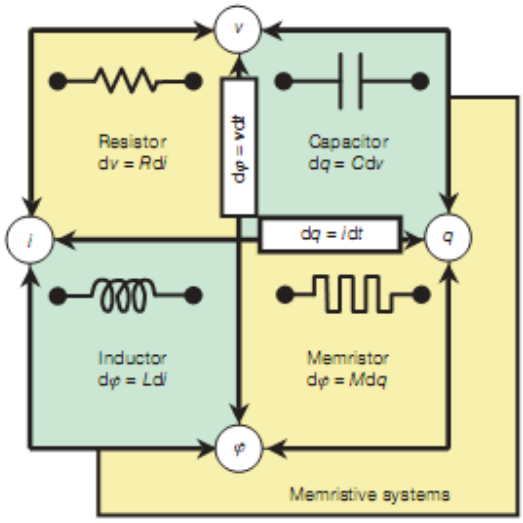

Figure 5.1 The four fundamental circuit elements

Where Q is defined by I = dQ/dt, and Φ_m is defined by V = $d\Phi_m$/dt. Note that the above table covers all meaningful ratios of I, Q, Φ_m, and V. No device can relate I to Q, or Φ_m to V, because I is the derivative of Q and Φ_m is the integral of V.

The variable Φ_m ("magnetic flux linkage") is generalized from the circuit characteristic of an inductor. It *does not* represent a magnetic field here, and its physical meaning is discussed below. The symbol Φ_m may simply be regarded as the integral of voltage over time.

Thus, the memristor is formally defined as a two-terminal element in which the flux linkage (or integral of voltage) Φ_m between the terminals is a function of the amount of electric charge Q that has passed through the device. Each memristor is characterized by its memristance function describing the charge-dependent rate of change of flux with charge.

$$M(q) = \frac{\mathrm{d}\Phi_m}{\mathrm{d}q} \tag{5.3}$$

Substituting that the flux is simply the time integral of the voltage, and charge is the time integral of current, we may write the more convenient form

$$M(q(t)) = \frac{\mathrm{d}\Phi_m/\mathrm{d}t}{\mathrm{d}q/\mathrm{d}t} = \frac{V(t)}{I(t)} \tag{5.4}$$

It can be inferred from this that memristance is simply charge-dependent resistance. If $M(q(t))$ is a constant, then we obtain Ohm's law $R(t) = V(t)/ I(t)$. If $M(q(t))$ is nontrivial, however, the equation is not equivalent because $q(t)$ and $M(q(t))$ will vary with time. Solving for voltage as a function of time we obtain

$$V(t) = M(q(t))I(t) \tag{5.5}$$

This equation reveals that memristance defines a linear relationship between current and voltage, as long as M does not vary with charge. Of course, nonzero current implies time varying charge. Alternating current, however, may reveal the linear dependence in circuit operation by inducing a measurable voltage without net charge movement as long as the maximum change in q does not cause much change in M.

Furthermore, the memristor is static if no current is applied. If $I(t) = 0$, we find $V(t) = 0$ and $M(t)$ is constant. This is the essence of the memory effect.

The power consumption characteristic recalls that of a resistor, I^2R.

$$P(t) = I(t)V(t) = I^2(t)M(q(t)) \tag{5.6}$$

As long as $M(q(t))$ varies little, such as under alternating current, the memristor will appear as a constant resistor. If $M(q(t))$ increases rapidly, however, current and power consumption will quickly stop.

5.3 Review of experimental research work

Because of interesting structure and properties of nanoparticles, they have a strong attention of researcher in various field including memory devices. Yang *et al.* [55] shows two types of device architectures. One has a triple layer structure sandwiched between two Al electrodes. The top and bottom layers of the triple-layer structure are made up of organic semiconductors, which have a thickness of 20-50 nm, whereas they used Al as the middle layer. Beside the metal nanoparticles, core shell CdSe/ZnS nanoparticles were also reported as the middle layer of the triple-layer structure by F. Li. *et al.* [58]. Another device structure has single layer sandwiched between two metal electrodes. Ouyang *et al.* [18] were the first to report such devices in 2005. Au nanoparticles capped with dendrons were also used in the single layer devices by Kim *et al.* [25]. Resistive switches were also observed on devices with semiconductor nanoparticles such as ZnO, ZnS, CdS, CdSe, and core shell CdSe/ZnS [51, 54].

Bipolar switching has been experimentally observed in various material systems such as organic films Scottand *et al.* [15]. Scottand reported typical hysteresis I-V curve which shows the memristic behavior. Strukov *et al.* [56] fabricate the device in which critical 5 nm thick oxide film initially contained one layer of insulating TiO_2 and one layer of oxygen-poor TiO_{2-x}. According to him, oxygen vacancies act as mobile +2 charged dopants which drift on the application of electric field giving hysteresis.

5.4 Present work

Inspired by the encouraging work by many peoples, an electrochemical device is fabricated as discussed below to investigate the switching properties of the fabricated nanoparticles.

5.4.1 Experimental details

Four-probe method is used for analyzing the switching behavior of nanoparticles. Four very thin wires of Cu are used as electrodes. A small piece of printed circuit board (PCB) and glass slide (having thin film over it), are pasted on a glass slide (as shown in fig 5.2) such that

there exists no gap between sample and PCB. Two terminals are made on PCB by using wet soldering. On both terminal two-two thin wires of copper are soldered. The contacts between the terminals and sample are made by using silver paste, which acts as electrodes. For analyzing, we use high precision 8-bit calibrator and high precision 8-bit multimeter. Calibrator is used for supplying DC voltage, while multimeter is used for recording current. One of the wires from first terminal of the PCB is connected to the high end of calibrator, while other wire is connected to the high of multimeter. Similarly the two wire from the other terminal of the PCB are connected to the low point of calibrator and multimeter respectively as shown in figure. The data so obtained is plotted. The voltage is given in mV, which in turns gives the current in mA. The above procedure is repeated for all the samples.

Figure 5.2 Experimental set-up for measuring I-V curve of ZnS samples

5.4.2 Results

For memristor, any asymmetrical alternating current voltage bias results in double-loop current-voltage hysteresis that collapses to straight line for high frequencies (figure 5.3). If there is any sort of asymmetry in the applied bias, multiple continuous states are obtained. Thus for DC voltages, the current voltage characteristics may be expected to exhibit hysteresis and for

successive observations, multiple loops may be expected. However we did not get multiple loops for successive observations.

The hysteretic I-V characteristics detected in the above samples can be understood as memristive behaviour defined by coupled equations of motion: some for (ionized) atomic degrees of freedom that define the internal state of device and others for the electronic transport. Due to this even on the application of small voltage in the range of mV, causes movement of charged species, which results into drastic change in current. It is evident from the I-V characteristics of all the samples that on the application of voltage in the range of -200 to 200mV there is no significant current but as we apply voltage above 220 mV, there is a drastic change in the current specification of the device. It increases abruptly at this point and increases continuously after that point up to 400 mV. After that point there is no change in current specification on further application of voltage increment. i.e. saturation point is obtained after that we apply voltage in reverse direction and procedure is repeated for taking the data.

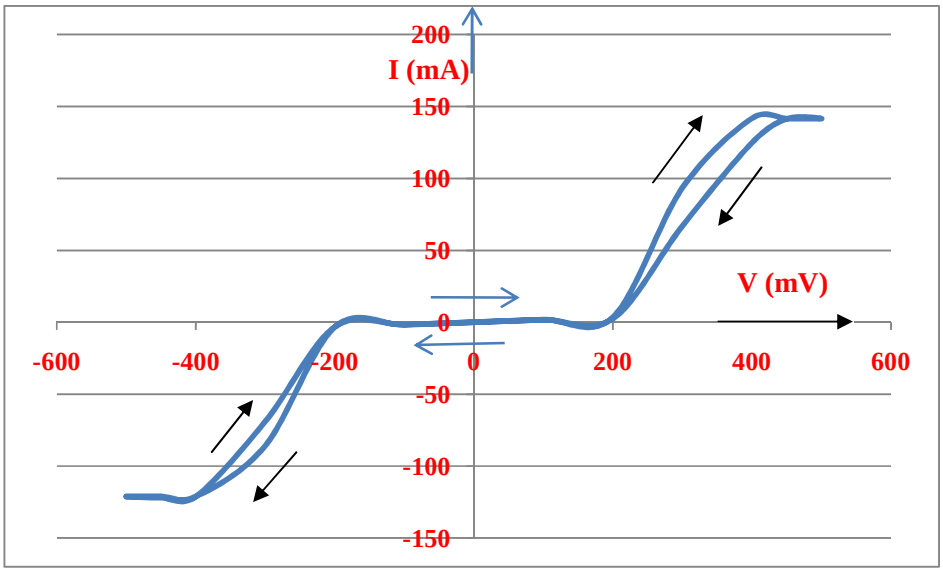

Figure 5.3 V-I curve for sample no 1

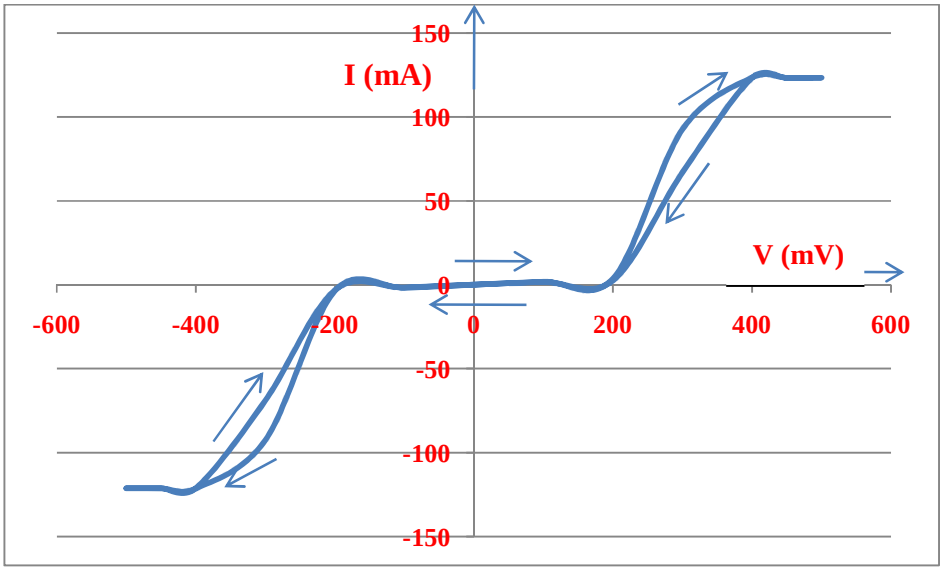

Fig 5.4 V-I curve for sample no 2

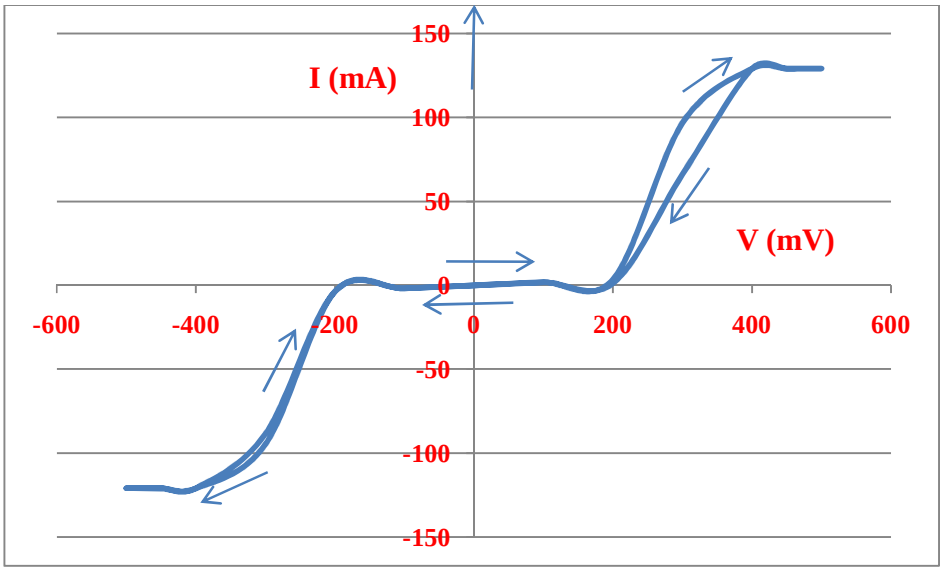

Fig 5.5 V-I curve for sample no 3

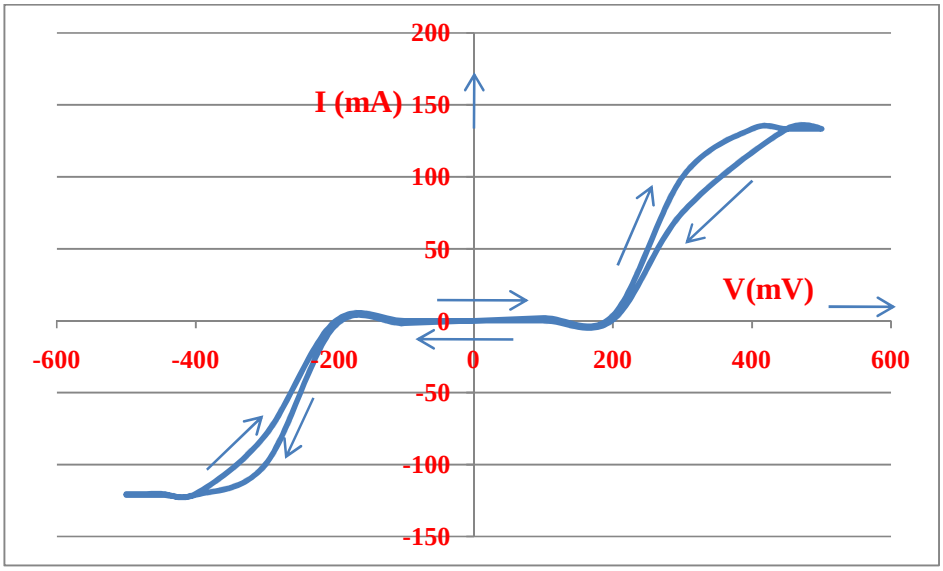

Fig 5.6 V-I curve for sample no 4

The current-voltage curve shows that the conductivity of the sample is low as compared to similar experiments done earlier by other workers. This may be because of less tunneling current in the present experiment due to larger dimension of non-conducting matrix compared to earlier experiments and due to absence of excitation from laser source. Conductivity may also be improved by using conducting polymer for the matrix.

All the samples show hysteresis as explained earlier. Along with hysteresis, we have also obtained binary switching property which is similar to that modeled by Strukov *et al.* [56]. In all the samples the current starts decreasing after attaining its maximum value and the saturation region in all these samples is very narrow. The curve clearly shows the switching property.

Another interesting feature of the I-V curves is their frequency behaviour. This is a manifestation of the fact that at low frequencies our system behaves essentially as a non-linear resistor. Physically, at low applied voltage frequencies, the electron spin polarization in the semiconductor has enough time to adjust to any present value of the voltage. Therefore, the current through the system at low frequency is non linear because of spin-blockade but essentially history independent (no hysteresis).

5.3 Conclusion

The samples of ZnS embedded in PVOH matrix are found to be exhibit switching properties. The general behaviour of the samples is found to be retained. Nanoparticles of ZnS samples show low conductivity. This is due to non conducting matrix of PVOH. The concept for application of the nanocomposites fabricated as switching as well as memristive device is developed in the present work and with advanced technological facilities for device fabrication from these samples can be developed for relevant applications in the field of electronics

CHAPTER 6

General conclusion and future direction of present work

Chapter 6

General conclusion and future direction of present work

6.1 Conclusion

In the present investigation, ZnS nanoparticles are fabricated embedded in PVOH matrix by adopting chemical route. The chemical route was chosen and each fabrication process is carried out by varying various physical parameters such as rotation per minute, temperature, and time duration and weight ratio.

Chemical characterization results confirm quantum confinement. Photoluminescence spectra peaks originating from near band edge emission, intrinsic defects states as well as extrinsic defects levels. Chemical composition of the fabricated sample is confirmed by the EDS analysis.

Structural characterization done by XRD gives size around 7 nm and the structure to be hexagonal. Other structural characteristics such as d-value of the lattice planes obtained from XRD matches with the standard JCPDS data.

Luminescence spectroscopy discloses the idea and possibilities of nanoparticles to act as LED. For luminescence in the visible range, intrinsic and extrinsic defects levels are more important. In the present study, suitable luminescence peaks for such defects levels are observed for the samples.

The samples of ZnS are found to have switching properties. Thus the concept for application of the nanocomposites in the present work and with advanced technological facilities suitable devices with these samples can be developed for applications as LED, switch and memory unit in the field of electronics.

6.2 Future work

With different matrix, the whole investigation can be repeated for getting better characteristics, if possible, for application as LED, electronic switch and memristor. Moreover, for reducing the resistivity for switch as well as for memristor applications, non conducting matrix can be replaced by conducting matrix. Charge storage in semiconductor nanoparticles can result into resistive switches. These devices can be switched between ON and OFF states for numerous times and have good stability in both cases. This renders the strong application of these devices as the two terminal memory devices. They can have extensive application in both high and low-end systems.

However fully exploring all the advantages of these devices will consume time and needs close collaborations among the material scientists, chemists and physicists. For example, one big problem in these devices is the repeatability, arising from the difficulties in precisely controlling the sizes of the nanoparticles. There is also technical difficulty in preparing thin films uniformly dispersed with nanometer materials. In addition the electrical conductivity of nanoparticles strongly depends on the experimental conditions. Thus, laboratories sometimes reported quite different data in the resistance ratio of OFF to ON, endurance and retention time of the devices. It is believed that all these problems will be solved with the rapid development of nanoscience and nanotechnologies in future.

References:

[1] S. V. Gaponeko, *Optical properties of semiconductor nanoparticles.* (Cambridge University Press, 1998).

[2] C. Delerue and M. Lannoo, *Nanostructures: Theory and Modeling*, (Springer, 2004).

[3] W. R. Fahrner, *Nanotechnology and Nanoelectronics* (Springer, 2005).

[4] A.D. Yoffe, *Adv. In Physics* **51**, 799 (2002).

[5] Wikipedia *http://en.wikipedia.org/wiki/Nanoparticle*.

[6] J. Singh, *Semiconductor Devices*, (John Wiley & Sons, Inc. 2002).

[7] Charles P. Poole, Frank J. Owens, *Introduction to nanotechnology IEEE*, (2003).

[8] A. I. L. Efros and A. L. Efros, *Semiconductors,* **16,** 1209 (1982).

[9] J. G. Lu, Z. Z. Ye, J. Y. Haung, L. P. Zhu, B. H. Zhao, Z. L. Wang and Sz. Fujita, *Applied Physics Lett.* **88**, 063110 (2006).

[10] G. Cao., *Nanostructures and Nanomaterials: Synthesis, properties & applications*, (Imperial college press, 1998).

[11] M. Lundstrom, *Science* **299,** 210 (2003).

[12] M. Hosokawa, K Naito, and T. Yokoyama (Ed.), *Nanoparticle Technology Handbook*, (Elsevier, 2007).

[13] R. N. Bhargava, D. Gallagher, X. Hong and A. Nurmikko, *Physics Rev. Lett.* **72,** 416 (1994).

[14] L. Xiao, Z. Chen, C. Feng., L. Liu, Z. Q. Bai, Y. Wang, L. Qian, Y. Zhang, Q. Li, K. Jiang and S. Fan, *Nano Lett.* **8,** 4539 (2008).

[15] J. C. Scottand and L. D. Bozano, *Adv. Mater.* **19,** 1452 (2007)

[16] L. O. Chua, *IEEE Trans. Circuit Theory.* **18,** 507 (1971).

[17] *http://en.wikipedia.org/wiki/Zinc_sulfide*

[18] J. Ouyang, W. Chu, C. Szmanda, L. Ma, and Y. Yang, *Nat. mater*.**3,** 918 (2004).

[19] W. G. Becker, and A. J. Bard, *J. Phys. Chem.* **87,** 4888 (1983).

[20] Y. Yang, J. Haung, S. Liu and J. Shen, *J. Material Chemistry* **7,** 131 (1997).

[21] W. Chen, Z. Wang, Z. Lin and L. Lin, *J. Applied Physics* **82,** 3111 (1997).

[22] J. Xu and W. Ji, *J. Material Science Lett.* **18,** 115 (1999).

[23] R. Passler, E. Griebl, H Riepl, G. Lautner, S. Bauer, H. Presis, W. Gabhardt, B. Buda, D. J. As, D. Schikora, K. Lischka, K. Papagelis, and S. Ves, *J. Appl. Phy*. **86,** 4403 (1999).

[24] S. B. Qadri, E. F. Skelton, D. Hsu, A. D. Dinsmore, J. Yang, H. F. Gray and B. R. Ratna, *Phys. Rev. B* **60,** 9191 (1999).

[25] C. K. Kim, W. J. Joo, H. J. Kim, E. S. Song, J. Kim and S. Lee, *Synth. Met.* **158,** 359 (2008).

[26] C. Ma, D. Moore, J. Li and Z. L. Wang, *Adv. Mater*. **15,** 228 (2003).

[27] I. Chakraborty and S. P. Moulik, *J. Dispersion Sci. And Tech.* **25,** 849 (2004).

[28] S. C. Ghosh, C. Thanachayanont and J. Dutta, *ECTI Annual Conference,* Pattaya, Thailand, 145 (2004).

[29] Y. Ding, X. D, Wang and Z. L. Wang, *Chem. Phys. Lett.* **398,** 32 (2004).

[30] K. S. Rathore, D. Patidar, Y. Janu, N. S. Saxena, K. Sharma and T. P. Sharma, *Chalcogenide Lett.* **5,** 105 (2008).

[31] S.S Nath, D. Chakdar, G. Gope, J. Kakati, B. Kalita, A. Talukadar, and D. K. Avasthi, *J. Appl. Phys.* **105,** 094305 (2009).

[32] J. Tauc, *Amorphous and Liquid Semiconductors,* (Plenum, 1974).

[33] A. A. Khosravi, M. Kundu, B. A. Kuruvilla, G. S. Shekhawat, R. P. Gupta, A. K. Sharma, P. D. Vyas and S. K. Kulkarni, *Appl. Phys. Lett.* **67,** 2506 (1995).

[34] J. Haung, Y. Yang, S. Xue, B. Yang, S. Liu and J. shen, *Appl. Phys. Lett.* **70,** 2235 (1997).

[35] W. Que, Y. Zhou, Y. L. Lam, Y. C. Chan, C. H. Kam, B. Liu, L. M. Gan, C. H. Chew, G. Q. Xu, S. J. Chua, S. J. Xu, and F. V. C. Mendis, *Appl. Phys. Lett.* **73,** 2727 (19980.

[36] P. H. Borse, N. Deshmukh, R. F. Shinde, S. K. Date and S. K. Kulkarni, *J. Mater. Sci.* **34,** 6087 (1999).

[37] K. Jayanthi, S. Chawla, H. Chander and D. Haranath, *Crys. Res. Tech.* **42,** 976 (2007).

[38] P. Yang, and M. Bredol, *Research Lett. Mater. Sci.* **2008,** 506065(ID) (2008)

[39] A. Glocher, and S.I. Shah (Ed.), *Handbook of thin film processing technology,* D2.4 (IOP Publishing Ltd. 1995)

[40] H. Warad, A. Sugunan, S. C. Ghosh, C. Thanachayanont and J. Dutta, *Adv. Technol. Mater.* (2004).

[41] K. Borgohain and S. Mahamuni, *Semicond. Sci. Technol.* **13,** 1154 (1998).

[42] S. S. Nath, *Phd. Thesis,* Deptt. Of Phy., Tezpur University, Assam, India (2003)

[43] A. O. E. Animaleu, *Intermediate quantum theory of crystalline solids,* (Prentice Hall Of India, 1989)

[44] F. A. Vladimir, A. A. Khan, B. A. Alexander, X. Faxian and L. Jianlin, *Phys. Rev. B.* **73,** 165317 (2006).

[45] S. Jafri, S. Promnimit, C. Thanachayanont and J. Dutta, (2006).

[46] Visible and Ultraviolet Spectroscopy, Available at:

http://www.cem.msu.edu/~reusch/virtualtext/spectrpy/UV-Vis/spectrum.htm.

[47] S. Y. Chang, L. Liu, and A. Asher, *J. Am. Chem. Soc.* **116,** 6739 (1994).

[48] R. Bhadra, *Phd. Thesis,* Deptt. Of ECE, Guwahati University, Assam, India (2003).

[49] S K. Kulkarni *Nanotechnology: Principle and Practices.* Capital Publishing Agency (2008).

[50] N. Khumbhojkar, V. V. Nikesh, A. Kshirsagar and S. Mahamuni, *J. Appl. Phys.* **88,** 6260 (2000).

[51] R. Bhadra, V. N. Singh, B. R. Mehta and P. Datta *Chalconide Lett.Vol. 6,* **5,** (2009).

[52] H. Li, W. Y. Shih, and W. H. Shih, *Nanotechnology,* **18,** 205604 (2007).

[53] H. Tews, H. Venghaus and P. J. Dean, *Phys. Rev.B* **19,** 5178 (1979).

[54] J. Ouyang *Application of nanomaterials in two-terminal resistive-swithing memory devices, Nano reviews* (2010).

[55] Y. Yang, J. Ouyang, L. Ma, C. W. Chu and R. J. Tsung, *Adv. Funct. Mater,* **14,** 1001 (2006).

[56] D. B. Strukov, G. S. Snider, D. R. Stewart & R. S. Williams, *Nature Lett.* 06932 (2008).

[57] Memristor Available at: http://en.wikipedia.org/wiki/Memristor.

[58] F. Li, D. I. Son, J. H. Ham, B. J. Kim, H. J. Jung, W. T. Kim, *Appl. Phys. Lett.* **82,** 1419 (2007).